Title

Analysis of Mll1 deficiency identifies neurogenic transcriptional modules and Brn4 as a factor for direct astrocyte-to-neuron reprogramming.

Journal

Neurosurgery, 75(4)

ISSN

0148-396X

Authors

Potts, Matthew B
Siu, Jason J
Price, James D
et al.

Publication Date

2014-10-01

DOI

10.1227/neu.0000000000000452

Peer reviewed

Analysis of *Mll1*-deficiency identifies neurogenic transcriptional modules and *Brn4* as a factor for direct astrocyte-to-neuron reprogramming

Matthew B. Potts, MD,[1,4] Jason J. Siu, BS,[1,4] James D. Price, BS,[1,4] Ryan D. Salinas, MS,[1,4] Mathew J. Cho, BA,[1,4] Alexander D. Ramos, BS,[1,4] Junghyun Hahn, PhD,[2] Marta Margeta, MD, PhD,[2] Michael C. Oldham, PhD,[3,4] Daniel A. Lim, MD, PhD[1,4,5]*

[1]Department of Neurological Surgery, [2]Department of Pathology, [3]Department of Neurology, [4]The Eli and Edythe Broad Institute of Regeneration Medicine and Stem Cell Research at UCSF, [5]Surgical Service, San Francisco Veterans Affairs Medical Center.
University of California, San Francisco
San Francisco, CA, USA

*Corresponding author:
Daniel A. Lim, MD, PhD
35 Medical Center Way
San Francisco, CA 94143-0525
Email: limd@neurosurg.ucsf.edu
Phone: 415.476.8138
Fax: 415.514.2346

Disclosure of Funding: This work was supported by VA BSLRD Merit Award (1l01 BX000252), NIH New Innovator Award (DP2-OD00650), and a UCSF REAC/CTSI pilot award to Dr. Lim; NIH NSRA (1F32NS073173-01) to Dr. Potts; NIH grant (R01-NS073765) to Dr. Margeta; the UCSF Program for Breakthrough Biomedical Research, which is funded in part by the Sandler Foundation, to Dr. Oldham; and facilities and resources provided by the San Francisco Veterans Affairs Medical Center. The authors declare no competing financial interest.

Analysis of *Mll1*-deficiency identifies neurogenic transcriptional modules and *Brn4* as a factor for direct astrocyte-to-neuron reprogramming

ABSTRACT

BACKGROUND: *Mixed lineage leukemia-1* (*Mll1*) epigenetically regulates gene expression patterns that specify cellular identity in both embryonic development and adult stem cell populations. In the adult mouse brain, multipotent neural stem cells (NSCs) in the subventricular zone (SVZ) generate new neurons throughout life and *Mll1* is required for this postnatal neurogenesis but not for glial cell differentiation. Analysis of *Mll1*-dependent transcription may identify neurogenic genes useful for the direct reprogramming of astrocytes into neurons.

OBJECTIVE: To identify *Mll1*-dependent transcriptional modules and determine whether genes in the neurogenic modules can be used to directly reprogram astrocytes into neurons.

METHODS: We performed gene coexpression module analysis on microarray data from differentiating wild-type and *Mll1*-deleted SVZ NSCs. Key developmental regulators belonging to the neurogenic modules were overexpressed in *Mll1*-deleted cells and cultured cortical astrocytes, and cell phenotypes were analyzed by immunocytochemistry and electrophysiology.

RESULTS: Transcriptional modules that correspond to neurogenesis were identified in wild-type NSCs. Modules related to astrocytes and oligodendrocytes were enriched in *Mll1*-deleted NSCs, consistent with their gliogenic potential. Overexpression of genes selected from the neurogenic modules enhanced the production of neurons from *Mll1*-deleted cells, and the overexpression of *Brn4 (Pou3f4)* in non-neurogenic cortical astroglia induced their transdifferentiation into electrophysiologically active neurons.

CONCLUSIONS: Our results demonstrate that *Mll1* is required for the expression of neurogenic – but not gliogenic – transcriptional modules in a multipotent NSC population and further indicate that specific *Mll1*-dependent genes may be useful for direct reprogramming strategies.

KEYWORDS: Astrocytes, *Brn4 (Pou3f4)*, Cell Transdifferentiation, Epigenomics, *Mll1*, Neural Stem Cells, Neurogenesis

RUNNING TITLE: *Mll1*-dependent neurogenic transcription and reprogramming

INTRODUCTION

In the adult mammalian brain, neural stem cells (NSCs) in the lateral ventricle subventricular zone (SVZ) continue to generate new neurons and glia throughout life.[1-6] In mice, SVZ NSCs are a specialized type of astrocyte that can produce both neuronal and glial cell lineages.[7] *Mixed lineage leukemia-1 (Mll1)* encodes an evolutionarily conserved chromatin-modifying factor that is required to maintain lineage-specific gene expression in both embryonic and postnatal stem cell populations.[8,9] In SVZ NSCs, *Mll1* is required for neurogenesis but not for glial cell differentiation.[7,10] Thus, *Mll1*-dependent gene expression may in part account for the neurogenic potential of this specialized population of astrocytes in the adult mouse SVZ.

Interestingly, astrocytes derived from non-neurogenic brain regions such as the cerebral cortex can be directly converted into functional neurons via the overexpression of specific transcription factors.[1,3,5,6,11] For instance, enforced expression of *Dlx2, Mash1 (*also known as *Ascl1)*, or *Pax6* in cultured postnatal mouse cortical astroglia results in neuronal transdifferentiation.[1,3,5,6] Furthermore, emerging evidence indicates that direct astrocyte-to-neuron reprogramming can also be achieved *in vivo*,[12,13] as is seen in striatal astrocytes where lentiviral transduction of *Sox2* along with the expression of specific extrinsic signals results in the production of mature neurons.[12] Given the astrocytic identity of SVZ NSCs, we hypothesized that characterizing their neurogenic gene expression profile may reveal new factors useful for reprogramming astrocytes into neurons.

Genome-wide analysis of *Mll1*-dependent transcription in SVZ NSCs provides an excellent opportunity to distinguish neurogenic gene expression from that required for glial cell differentiation. While wild-type SVZ NSCs produce all three major neural cell types – neurons, astrocytes, and oligodendrocytes – *Mll1*-deficient SVZ cells efficiently generate only the glial lineages.[10] However, our understanding of *Mll1*-dependent gene expression has been limited. Proneural *Mash1* and gliogenic *Olig2* are expressed in *Mll1*-deficient SVZ cells during differentiation but *Dlx2* is not expressed, correlating with the impaired neurogenesis.[10]

In this study, we used microarrays and gene coexpression analysis to identify "modules" of transcribed genes that distinguish neurogenesis from gliogenesis. In

contrast to differential gene expression analysis, which compares the mean expression level of individual genes between two or more groups, gene coexpression analysis seeks to identify groups of genes (*i.e.,* transcriptional modules) that are expressed in similar patterns across biological samples.[14-17] Such approaches enable the discovery of cell type-specific gene expression despite cellular heterogeneity within each sample.[14,16]

Our coexpression analysis generated a resource that distinguishes gene expression modules related to SVZ neurogenesis from those related to gliogenesis and cell proliferation. To evaluate the neurogenic potential of genes identified by this method, we used lentiviruses to overexpress select module members in *Mll1*-deficient SVZ cells. Using this approach, we identified genes such as *Brn4* (also known as *Pou3f4*) that belonged to neurogenic modules and partially rescued neuronal differentiation. Finally, to explore whether *Mll1*-dependent genes in SVZ NSCs can be used to transdifferentiate non-neurogenic astrocytes into neurons, we overexpressed *Brn4* in astrocytes cultured from the cerebral cortex. We observed that the overexpression of *Brn4* in cortical astrocytes resulted in the production of electrophysiologically active neurons. Taken together, these studies provide insight into the key role that *Mll1* plays in postnatal neurogenesis and further indicate that neurogenic factors expressed in SVZ NSCs may be useful for astrocyte-to-neuron reprogramming strategies.

MATERIALS AND METHODS

Tissue preparation and culture of primary SVZ NSCs and cortical astrocytes

All use of animals was performed in accordance with guidelines established by the Institutional Animal Care and Use Committee at the University of California, San Francisco. *Mll1*-deleted SVZ NSCs were obtained from *hGFAP-Cre;Mll1*$^{f/f}$ mice, which exhibit Cre-mediated recombination of the *Mll1*$^{f/f}$ alleles in cells expressing the *hGFAP-Cre* transgene. *hGFAP-Cre;Mll1*$^{+/+}$ litter mates were used as wild-type controls. The brains from mice aged postnatal days 5-7 were removed from the skull and placed in ice-cold Leibovitz's L15 media (Gibco, Cat. No. 11415-064). Coronal slabs containing the SVZ were obtained and the meninges removed. The lateral SVZ and cortical gray matter were then microdissected with care taken to prevent cross-contamination. Dissected tissue was then dissociated with 0.25% trypsin as previously described.[10] The suspension

of cortical astrocytes was also treated with DNase I (Roche Diagnostics, Cat. No. ROCZR139). SVZ single cell suspensions were plated in "N5" medium[18] containing DMEM/F12 with Glutamax (Gibco, Cat. No. 10565-018), 5% fetal bovine serum (FBS; Hyclone, Cat. No. SH30070.03), N2 supplement (Gibco, Cat. No. 17502-048), 35μg/ml bovine pituitary extract (BPE; Gibco, Cat. No. 13028.014), 20ng/ml recombinant human epidermal growth factor (EGF; Peprotech, Cat. No. AF-100-15), 20ng/ml recombinant human fibroblast growth factor (FGF; Peprotech, Cat. No. 100-18B-1mg), and antibiotic-antimycotic (Gibco, Cat. No. 15240-062). SVZ cultures were maintained with serial passages as previously described.[18] At the first or second passage, SVZ cells were seeded onto 16-well chamber slides and immunostained for mouse MLL1 (1:500; Millipore, Cat. No. 05-764) to confirm ≥90% deletion before proceeding with RNA isolation for subsequent experiments. Cortical astrocyte single cell suspensions were resuspended in medium containing DMEM/F12, 10% FBS, 5% horse serum (UCSF Cell Culture Facility, Cat. No. CCFAW001), B27 supplement (Gibco, Cat. No. 17504-044), 3.5mM glucose, 10ng/ml EGF, 10ng/ml FGF, and antibiotic-antimycotic. Astrocytes were then plated on culture dishes pre-coated with 0.1mg/ml poly-D-lysine (PDK; Sigma-Aldrich, Cat. No. P6407) and 2μg/ml laminin (Life Technologies, Cat. No. 23017-015) and allowed to reach confluence.

SVZ cultures were differentiated after 5-7 passages. For differentiation, the medium was changed to a serum-free differentiation medium consisting of DMEM/F12 with Glutamax, N2 supplement, BPE, and antibiotic-antimycotic.[18] Astrocyte differentiation was performed after the first passage by changing to a medium consisting of DMEM/F12, 3.5mM glucose, B27 supplement, antibiotic-antimycotic, and 20ng/ml of brain derived neurotrophic factor (BDNF; Peprotech, Cat. NO. 450-02).

RNA isolation and microarray analysis

Microarray analysis of wild-type and *Mll1*-deleted SVZ NSC cultures was performed pre-differentiation (0 days) and at 1, 2, and 4 days after differentiation (biologic triplicates at each time point). SVZ cultures were homogenized using QIAshredder columns (QIAgen, Cat. No. 79654) and RNA was extracted using QIAgen RNeasy Plus Mini Kit (Cat. No. 74134). RNA quality and integrity were assessed with

the Agilent BioAnalyzer 2100 before samples were converted to cDNA. Affymetrix Mouse Gene 1.0 ST microarrays were used to measure gene expression levels and scanned by the UCSF Genomics Core. Raw data (.CEL files) were pre-processed using the Affymetrix Power Tools (APT) software package (http://www.affymetrix.com/partners_programs/programs/developer/tools/powertools.affx). Expression data were background-corrected, summarized, and quantile-normalized using the robust multi-array average (RMA) algorithm[19] in APT. Sample heterogeneity was assessed using the SampleNetwork R function;[20] the mean inter-sample adjacency was 0.968 and no outliers ($Z.K < -3$) were present.

Gene coexpression analysis

Gene coexpression modules were identified using a four-step approach. First, pairwise Pearson correlation coefficients (cor) were calculated across all samples for all transcripts (n = 25,232) that were perfectly and uniquely targeted by their microarray probe sequence (Affymetrix 'CrossHyb Type' = 1). Second, transcripts were clustered using the flashClust[17] implementation of a hierarchical clustering procedure with complete linkage and 1 – cor as a distance measure. The resulting dendrogram was cut at a static height of ~0.258, corresponding to the top 1% of pairwise correlations for the entire dataset. Third, all clusters consisting of at least 15 members were identified and summarized by their module eigengene (*i.e.*, the first principal component obtained via singular value decomposition).[14,15] Fourth, highly similar modules were merged if the Pearson correlation coefficients of their module eigengenes exceeded an arbitrary threshold (0.85). This procedure was performed iteratively such that the pair of modules with the highest correlation > 0.85 was merged, followed by recalculation of all module eigengenes, then followed by recalculation of all correlations, until no pairs of modules exceeded the threshold. Following these steps, 14 coexpression modules were identified. The strength of module membership (kME) for each probe on the microarray was calculated by correlating its expression pattern across all samples with each module eigengene.[15,16]

Module enrichment analysis

Module enrichment analysis with curated gene sets was performed using a one-sided Fisher's exact test for over-representation with gene symbols as a common identifier. Curated gene sets included experimentally validated markers of astrocytes (Table S7 from Bachoo et al.[21]), oligodendrocytes (from Nielsen et al.,[22] reanalyzed as previously described;[16] from Cahoy et al.,[23] restricted to genes expressed >10X higher in oligodendrocytes versus other cell types in the adult mouse forebrain; and from Doyle et al.,[24] consisting of markers of mouse cerebellar Olig2+ oligodendrocytes), and neurons (from Cahoy et al.,[23] restricted to genes expressed >10X higher in neurons versus other cell types in the adult mouse forebrain). Modules were defined as consisting of all transcripts that were positively correlated with the module eigengene at a significance threshold of $P<1.26e^{-07}$. This threshold corresponds to a Bonferroni-corrected *P*-value of .05 / (the total number of probes X the total number of modules). Gene Ontology (GO, http://www.geneontology.org) analysis was performed using DAVID (Database for Annotation, Visualization, and Integrated Discovery, http://david.abcc.ncifcrf.gov/). Probe IDs of module genes were uploaded and converted to gene lists using as a background all transcripts (n = 25,232) that were perfectly and uniquely targeted by their microarray probe sequence (Affymetrix 'CrossHyb Type' = 1). To determine if modules were *Mll1*-dependent or independent, analysis of variance (ANOVA) was performed in R (http://cran.us.r-project.org/) on multivariate linear regression models that related each module eigengene to treatment condition (wild-type versus *Mll1*-deleted), the number of days in culture, and the interaction between these two terms. *Mll1*-dependence was defined as $P<0.05$ for the treatment effect.

Enforced expression of *Mll1*-dependent factors

cDNA of genes of interest (*Dlx2, Brn4, Tlx, Zdhhc23*, and *Shisa3*) was cloned into the lentiviral pUltra vector (Addgene), which contains a green fluorescent protein (GFP) reporter. Lentivirus was then generated from HEK293T cells with 36µg of plasmid containing a given cDNA of interest, 9µg VSVg coat plasmid, 7.5µg pRSV, and 7.5µg pMDL helper plasmids using the FuGENE 6 transfection system (Promega, Cat. No. E2693). One day after transfection, cell culture media was changed to viral production media containing Lonza Ultraculture media (12-1725F), 110ng/mL sodium

pyruvate, and 5mM sodium butyrate. Cells were grown in viral production media for 48 hours before pelleting of virus at 22,000 rpm by ultracentrifuge for 2 hours. Viral pellet was resuspended in PBS and stored at -80° Celsius.

Immunocytochemistry

At the time points of interest, cells were fixed in 4% paraformaldehyde for 30 minutes and then washed three times in phosphate buffered saline (PBS). Blocking was performed for 2 hours at room temperature in blocking buffer containing PBS with 1% bovine serum albumin, 5% normal goat serum, 0.3% Triton-X-100 (Sigma), 0.3 M glycine, and 0.03% sodium azide. All antibody incubations were also performed in blocking buffer at room temperature. Primary antibodies included mouse anti-neuronal class III ß-tubulin (Tuj1, 1:500; Covance, Cat. No. MMS-435P), mouse anti-microtubule associated protein 2 (MAP2, 1:200; Millipore, Cat. No. MAB364), guinea pig anti-doublecortin (DCX, 1:400; Millipore, Cat. No. AB2253), rabbit anti-Brn4 (1:500; Millipore, Cat. No. AB15456), rabbit anti-glial fibrillary acidic protein (GFAP, 1:500; Dako, Cat. No. Z0334), chicken anti-GFP (1:500; Aves, Cat. No. GFP-1020), mouse anti-O4 (1:100; Millipore, Cat. No. MAB345), rabbit anti-NG2 (1:400; Millipore, Cat. No. AB5320), mouse anti-GAD67 (1:1000; Millipore, Cat. No. MAB5406), and rabbit anti-Calbindin (CalB, 1:200; Swant, Cat. No. CB 38). Appropriate secondary antibody incubations were performed for 30 minutes in blocking buffer at room temperature and included a nuclear counterstain (DAPI). Imaging was performed using a Leica DMA4000 B inverted fluorescent microscope. Cell counts for a given condition were performed on seven non-overlapping regions imaged at 20X. The totals of each region were then summed and averaged over biological triplicates.

Electrophysiology

Whole-cell current-clamp recordings[25] were made using a Multiclamp 700B amplifier (Molecular Devices, CA, USA). Signals were filtered at 1 kHz and sampled at 10 kHz using a Digidata 1440A analog-to-digital converter (Molecular Devices). All data were recorded and analyzed with pClamp 10 software (Molecular Devices). The liquid junction potential was measured with 3 M KCl and adjusted. Cells on coverslips

were placed in a bath solution (containing the following in mM: 135 NaCl, 5 KCl, 2 CaCl2, 1.2 MgCl2, 10 HEPES, 10 glucose at ~300 mOsm [pH 7.4]) and visualized using an Olympus IX71 microscope with differential interface contrast optics at 40X. Patch electrodes (3-4 MΩ) contained (in mM) 125 KCl, 10 Na_2PO_4, 10 HEPES, 2 Mg3ATP, 0.3 Na2GTP at ~ 290 mOsm (pH 7.4). Currents were manually injected to hold the membrane potential around -70 mV to record voltage responses. Tetrodotoxin (TTX, 1 μM; Tocris, Cat. No. 1078) was applied through a gravity-fed perfusion system.

RESULTS

Mll1 is required for the expression of transcriptional modules related to SVZ neurogenesis.

In the adult and postnatal mouse brain, SVZ NSCs produce neuroblasts that migrate to the olfactory bulb where they differentiate into interneurons and integrate into local circuits.[26,27] SVZ NSCs can also generate astrocytes in response to local injury[28] as well as oligodendrocytes in both normal and pathologic conditions.[29-31] When cultured as monolayers, SVZ NSC cultures express Nestin and Sox2[10,18] and can recapitulate the development of these distinct neural lineages,[10,18,32] with wild-type SVZ NSCs efficiently generating neurons, astrocytes, and oligodendrocytes (Figure 1A). In contrast, *Mll1*-deleted SVZ NSCs (which are derived from *hGFAP-Cre;Mll1$^{f/f}$* mice and are ~95% deleted for *Mll1*[10]) survive, proliferate, and produce glia, but are defective for neurogenesis (Figure 1B).[10] To identify *Mll1*-dependent gene expression, we performed microarray analysis of wild-type and *Mll1*-deleted SVZ cultures in self-renewal conditions and after 1, 2, and 4 days of differentiation (each performed in biological triplicate). By analyzing gene coexpression relationships,[14-16] we identified 14 transcriptional "modules" (labeled by color), each representing groups of genes with expression levels that were highly correlated across the 24 samples (Supplementary Figure 1 and selected modules in Figure 2A). Each module was related to specific biological processes and neurobiological cell types via enrichment analysis for GO terms (Table 1) and curated biological gene sets.

Seven of the 14 coexpression modules exhibited similar temporal patterns in wild-type and *Mll1*-deleted cells, indicating that some SVZ gene expression programs do not

require *Mll1* (Supplementary Table 1). For example, the turquoise module (Figure 2B) consisted of genes that were progressively down-regulated under differentiation conditions in both wild-type and *Mll1*-deleted cells. This module was highly enriched for GO terms related to cell cycle regulation (Table 1) and these findings are consistent with the observation that *Mll1*-deleted cultures proliferate at rates similar to wild-type SVZ NSCs.[10] The tan module (Figure 2B) consisted of genes that were quickly up-regulated under differentiation conditions in both wild-type and *Mll1*-deleted SVZ cells. This module contained *Gfap* and was enriched for experimentally validated markers of astrocytes[21] (P=2.76x10^{-8}); indeed, both *Mll1*-deleted and wild-type NSCs efficiently generate GFAP+ astrocytes.[10]

The greenyellow module consisted of genes with higher expression levels in *Mll1*-deleted cells versus wild-type cells at the 4 day time point (Figure 2B), and its relationship to oligodendrocytes was revealed by GO analysis (Table 1) and significant enrichment with experimentally validated markers of oligodendrocytes from Cahoy et al.[23] (P=1.11x10^{-29}), Nielsen et al.[22] (P=3.64 x 10^{-13}), and Doyle et al.[24] (P=3.02 x 10^{-14}). Interestingly, a trend towards increased oligodendrogliogenesis is observed with *Mll1*-deletion both *in vivo* and *in vitro*.[10]

Other coexpression modules exhibited temporal patterns of transcriptional upregulation that were strongly *Mll1*-dependent. For example, the black and magenta modules (Figure 2C) consisted of genes that were strongly upregulated in wild-type, but not *Mll1*-deleted, SVZ cells after 2 days (black) or 1 day (magenta) of differentiation (Supplementary Table 2). Both modules were enriched for GO terms related to neurogenesis (Table 1) and the black module was strongly significant for experimentally validated markers of mature neurons from Cahoy et al.[23] (P=2.77x10^{-15}). Black module gene members include *Dlx5, Dlx6, Sp8,* and *Sp9* – all of which encode transcription factors expressed in SVZ neuroblasts and olfactory bulb interneurons.[33,34] Furthermore, the presence of *Glutamic acid decarboxylase-1 (Gad1)* and *GABA(A) receptor-associated protein like 1* (*Gabarapl1*) in the black module suggest a GABAergic identity of neurons within the population of differentiating cells.

The magenta module contained genes that are expressed at earlier stages of neurogenesis (Supplementary Table 2). For instance, the expression of *Dlx1* generally

precedes that of *Dlx5* and *Dlx6*.[35] Consistent with this temporal relationship, *Dlx1* was a member of the magenta module, whereas *Dlx5* and *Dlx6* were members of the later-upregulated black module. *Dlx2*, which is also temporally expressed with *Dlx1,* was most strongly associated with the magenta module. Other magenta module genes included *Arx*, a homeobox transcription factor that regulates the proliferative expansion of immature neuronal progenitor cells in the developing cortex (*P*=3.45E-08),[36] and *Tlx* (also known as *Nr2e1*), which is required for SVZ NSC self-renewal.[37] Finally, *Brn4*, which has also been associated with SVZ neurogenesis,[38] was also identified in the magenta module.

Interestingly, at the time that the magenta module was first upregulated (1 day of differentiation), both wild-type and *Mll1*-deleted cultures lacked Tuj1-positive neuroblasts and contained many GFAP-positive astroglia (Figure 1). This early-differentiation expression of the magenta module suggests its relationship to early stages of neuronal lineage commitment in wild-type SVZ NSCs, which at that time still have astroglial characteristics.

Enforced expression of select magenta module genes partially rescues neurogenesis in *Mll1*-deleted SVZ cells.

To evaluate the neurogenic potential of genes associated with the magenta module, we tested their ability to rescue neuronal differentiation of *Mll1*-deleted SVZ cells. For each of these genes – *Dlx2, Tlx, Zdhhc23*, and *Brn4* – we generated an overexpression lentivirus that coexpresses the green fluorescent protein (GFP) marker (Table 2). To provide a negative control, we produced a lentiviral vector that expresses only the marker proteins GFP and alkaline phosphatase (LV-*hPLAP*-GFP). *Mll1*-deleted SVZ cultures were infected with each lentivirus, and after 4 days of differentiation, neuronal differentiation was assessed by immunocytochemistry (ICC, Figure 3A-F) and quantified (Figure 3G). In control virus-infected cultures (Figure 3A), approximately 10% of the GFP-positive cells were immunopositive for the Tuj1 neuronal marker (Figure 3G), representing the lower levels of neurogenesis of *Mll1*-deleted SVZ cells. As compared to this control, cultures infected with the *Dlx2* lentivirus (Figure 3B) resulted in a 5-fold increase in GFP-positive, Tuj1-positive cells (Figure 3G), which is similar to the rescue

previously observed with transient *Dlx2* overexpression.[10] Individual overexpression of *Brn4*, *Tlx,* and *Zdhhc23* also increased the production of neurons from *Mll1*-deleted SVZ cells (Figure 3C-E), albeit with approximately 2-fold lower efficiency than that of *Dlx2* (Figure 3G). We also generated a lentivirus that expresses *Shisa3*, a gene that was not found in the neurogenic modules, and infection with this vector did not significantly increase neuronal differentiation (Figure 3F and 3G). Thus, when overexpressed, select members of the magenta module can induce neurogenesis in *Mll1*-deleted SVZ cells.

Enforced expression of *Brn4* in cortically-derived primary astroglial cultures induces neurogenesis.

Astroglia cultured from the postnatal cortex can be transdifferentiated into neurons via the overexpression of certain single transcription factors including *Dlx2* and *Pax6*[1,3] – both of which are members of the magenta module. To test if another magenta module member could likewise induce neurogenesis from cortical astroglia, we enforced *Brn4* expression using LV-*Brn4*-GFP and analyzed the cell fate of GFP-positive cells after 20 days of differentiation. While *Brn4* has been associated with SVZ neurogenesis,[38] its ability to transdifferentiate astrocytes into neurons was unknown. As a control, we also followed the fate of astroglial cells infected with LV-*hPLAP*-GFP. Before *Brn4* overexpression, cortical astroglial cultures consisted of GFAP-positive cells (Figure 4A), and no Tuj1-positive neuronal cells were observed (data not shown). After 10 days of differentiation, LV-*Brn4*-GFP infected cultures contained GFP-positive, Tuj1-positive cells (data not shown). After 20 days of differentiation, these cultures contained GFP-positive, Tuj1-positive cells with neuronal morphology (Figure 4B). As expected, we did not observe any GFP-positive neuronal cells in the control LV-*hPLAP*-GFP infected cultures (quantified in Figure 4G). LV-*Brn4*-GFP infection also generated GFP-positive cells that co-expressed MAP2 (Figure 4C) or DCX (Figure 4D), further supporting the neuronal identity of these cells. In contrast, LV-*hPLAP*-GFP control infection did not produce any GFP-positive cells expressing the DCX and MAP2 neuronal antigens (quantified in Figure 4G). Furthermore, some neuronal cells induced by LV-*Brn4*-GFP expressed GAD67 (Figure 4E), an enzyme present in GABAergic neurons, and calbindin (Figure 4F), a marker of specific neuron subtypes. This ICC

analysis indicates that LV-*Brn4*-GFP infection induces the neuronal transdifferentiation of cortical astrocytes *in vitro*.

To further characterize the identity of these LV-*Brn4*-GFP induced neurons, we performed whole-cell patch clamp recordings (Figure 5). Resting membrane potential was recorded in current clamp mode without injecting current and found to be negative in each cell tested (-41 ± 2 mV, n=3), indicating the expression of ion channels and the regulation of ionic gradients across the cellular membrane. We then depolarized cells by injecting a series of depolarizing current steps and all cells tested fired action potentials that appeared after a threshold membrane potential in an all-or-none fashion (Cm = 28 ± 0.1 pA/pF, n=3, Figure 5B left). Additionally, these action potentials were reversibly eliminated by the addition of TTX, a specific blocker of voltage-gated Na^+ channels (Figure 5B middle and right). Taken together, these data indicate that neurons transdifferentiated from cortical astroglia via LV-*Brn4*-GFP infection are electrophysiologically functional.

DISCUSSION

The differentiation of neurons from multipotent NSCs requires the concerted expression of distinct sets of genes that promote neuronal identity. Such lineage-specific gene expression is in part coordinated by epigenetic regulators such as MLL1, a histone methyltransferase and member of the Trithorax group (TrxG) of chromatin regulators.[8,9] In human patients, *MLL1* mutations have been linked to Wiedemann-Steiner syndrome, a rare developmental disorder characterized by intellectual disability including autism.[39] We demonstrate that *Mll1* is required for the expression of neurogenic transcriptional modules in SVZ NSCs, indicating its central role in the gene expression required for normal neural development. Furthermore, genes selected from the neurogenic modules can promote neuronal differentiation from gliogenic cell populations. Our study thus provides new insights into the role that *Mll1* plays in neural development and further suggests that specific neurogenic module genes may be useful for direct astrocyte-to-neuron reprogramming strategies.

Mll1-deletion targeted to SVZ NSCs results in defective neurogenesis, and in a previous study, we found that this lineage-specific deficiency relates to the lack of proper

Dlx2 expression.[10] In the current study, we used microarray and gene coexpression analyses to further characterize the *Mll1*-dependent transcription that corresponds to neurogenesis. We identified two neurogenic gene coexpression modules – black and magenta – and our analysis suggests that the magenta module is involved in earlier stages of neuronal lineage commitment. The magenta module was upregulated in wild-type cultures after just 1 day of differentiation and before the appearance of Tuj1-positive neuroblasts, suggesting that gene expression in this module does not simply reflect transcription related to the presence of neurons. Indeed, *Dlx2*, which is most closely associated with the magenta module, is first expressed in SVZ transit amplifying cells, before their differentiation into Tuj1-positive migratory neuroblasts.[33] In addition, the magenta module defined 127 other genes with a similar pattern of expression (Supplementary Table 2), providing many novel candidates for the study of genes involved in early stages of neurogenesis.

Previously, we showed that transient overexpression of *Dlx2* partially rescues *Mll1*-dependent neurogenesis. For this study, we used lentiviral expression vectors to enforce the expression of *Dlx2, Tlx*, *Zdhhc23,* and *Brn4* in *Mll1*-deleted SVZ NSCs, and the resultant increase in neuronal differentiation induced by each vector demonstrated the neurogenic potential of these magenta module genes. Furthermore, the ability to induce neuronal differentiation of *Mll1*-deleted cells suggests that this TrxG chromatin regulator is not required for the transcription downstream of key neurogenic genes, at least when they are overexpressed.

Tlx encodes a nuclear receptor that is expressed in SVZ NSCs, and *Tlx*-deficiency reduces NSC self-renewal and SVZ neurogenesis.[37,40] Interestingly, transgenic overexpression of *Tlx in vivo* results in the expansion of the NSC population and glioma-like lesions;[40] it is therefore possible that the increased numbers of neurons observed with *Tlx* overexpression in *Mll1*-deleted cultures relates to increased proliferation of neurogenic progenitor cells. *Zdhhc23* encodes a zinc-finger-containing palmitoyl-transferase[41] that is associated with the synaptic membrane.[42] The function of this molecule is poorly understood, and, to our knowledge, it has not been previously associated with neurogenesis or *Mll1*.

Brn4 is a member of the POU domain transcription factor family. *Brn4* knock-out

mice exhibit deafness, vestibular abnormalities, and gait impairments.[43] *Brn4* is expressed in the SVZ of the adult rodent[44] and results of a recent study suggest that *Brn4* is a component of a transcriptional network downstream of *Pax6* that drives SVZ neurogenesis.[38] The *Brn4* locus is a direct target for the PAX6 transcription factor and *Pax6* overexpression upregulates *Brn4*.[38] Given this transcriptional interrelationship and the *Mll1*-dependence of *Pax6* expression, it is possible that the activation of the *Brn4* locus during neurogenesis is not directly dependent upon MLL1 and instead relates to activation by PAX6. Future studies of MLL1 protein enrichment and related chromatin state changes – as has been performed to demonstrate the role of MLL1 at the *Dlx2* locus[10] – will help clarify whether *Brn4* and other neurogenic genes are directly regulated by this chromatin-modifying factor.

Our study identified *Brn4* as a transcription factor that can induce neuronal transdifferentiation from cultured astrocytes. This finding contributes to the relatively small collection of factors that have been shown to promote the conversion of astrocytes into neurons.[1,3,5,6] *Pax6* can induce neurons from astrocytes, and, interestingly, this transcription factor was also a member of the magenta module. Similarly, *Dlx2*, which also induces neurons from astrocytes, was also most strongly associated with the magenta module. We did not detect *Ngn2* in an SVZ neurogenic module; however, the overexpression of *Ngn2* induces the production of glutamatergic neurons,[3] a cell type that is not commonly produced from SVZ NSCs. We also did not find *Mash1* as a member of a neurogenic module. Consistent with previous results, *Mash1* expression was not *Mll1*-dependent.[10] While *Mash1* overexpression induces transdifferentiation into GABAergic neurons, this transcription factor also plays a role in normal SVZ gliogenesis.[45] Recent studies of direct fibroblast-to-neuron reprogramming indicate that *Mash1* acts as a "pioneer" factor that promotes the recruitment of other transcription factors.[46] Indeed, astrocytes with both *Mash1* and *Dlx2* overexpression generate greater numbers of neurons than either transcription factor alone.[3] Future combinatorial strategies (e.g., *Mash1*, *Brn4,* and *Dlx2* together) may further improve the efficiency of neuronal reprogramming observed both *in vitro* and *in vivo.* Importantly, these findings may serve as a basis for future studies of neuronal reprogramming in human cells. Several studies have already demonstrated that human-derived cells can be successfully

reprogrammed.[47-49] Corti et al. have even converted human astrocytes into neurons using either OCT4, SOX2, or NANOG.[6] Interestingly, they also show that this process is epigenetically regulated through DNA methylation. Given the important role of *Mll1* in murine SVZ neurogenesis, it will be worthwhile to explore both its role in human neurogenesis and cell reprogramming. Neurosurgeons are in the unique position to do this through access to intraoperatively-derived human tissue.

CONCLUSION

This study provides new insights into the *Mll1*-dependent expression that underlies postnatal SVZ neurogenesis. Gene coexpression analysis identifies transcriptional modules that distinguish neurogenesis from gliogenesis, and enforced expression of select neurogenic factors can promote neurogenesis from *Mll1*-deleted SVZ NSCs. *Brn4* is identified as a factor for direct astrocyte-to-neuron transdifferentiation. These data thus serve as a resource for future studies of *Mll1* in neural development and direct astrocyte-to-neuron reprogramming strategies.

References

1. Heins N, Malatesta P, Cecconi F, et al. Glial cells generate neurons: the role of the transcription factor Pax6. *Nat Neurosci*. 2002;5(4):308–315. doi:10.1038/nn828.

2. Hwang WW, Alvarez-Buylla A, Lim DA. Glial Nature of Adult Neural Stem Cells: Neurogenic Competence in Adult Astrocytes. In: Rao MS, Carpenter M, Vemuri MC, eds. *Neural Development and Stem Cells*. Third Edition. Springer; 2012:149–172. doi:10.1007/978-1-4614-3801-4_6.

3. Heinrich C, Blum R, Gascón S, et al. Directing Astroglia from the Cerebral Cortex into Subtype Specific Functional Neurons. McKay RDG, ed. *PLoS Biol*. 2010;8(5):e1000373. doi:10.1371/journal.pbio.1000373.g015.

4. Fuentealba LC, Obernier K, Alvarez-Buylla A. Adult neural stem cells bridge their niche. *Cell Stem Cell*. 2012;10(6):698–708. doi:10.1016/j.stem.2012.05.012.

5. Heinrich C, Gascón S, Masserdotti G, et al. Generation of subtype-specific neurons from postnatal astroglia of the mouse cerebral cortex. *Nature Protocols*. 2011;6(2):214–228. doi:10.1038/nprot.2010.188.

6. Corti S, Nizzardo M, Simone C, et al. Direct reprogramming of human astrocytes into neural stem cells and neurons. *Exp Cell Res*. 2012;318(13):1528–1541. doi:10.1016/j.yexcr.2012.02.040.

7. Kriegstein A, Alvarez-Buylla A. The glial nature of embryonic and adult neural stem cells. *Annu Rev Neurosci*. 2009;32:149–184. doi:10.1146/annurev.neuro.051508.135600.

8. Schuettengruber B, Chourrout D, Vervoort M, Leblanc B, Cavalli G. Genome Regulation by Polycomb and Trithorax Proteins. *Cell*. 2007;128(4):735–745. doi:10.1016/j.cell.2007.02.009.

9. Zhang P, Bergamin E, Couture J-F. The many facets of MLL1 regulation. *Biopolymers*. 2013;99(2):136–145. doi:10.1002/bip.22126.

10. Lim DA, Huang Y-C, Swigut T, et al. Chromatin remodelling factor Mll1 is essential for neurogenesis from postnatal neural stem cells. *Nature*. 2009;458(7237):529–533. doi:10.1038/nature07726.

11. Berninger B, Costa MR, Koch U, et al. Functional Properties of Neurons Derived from In Vitro Reprogrammed Postnatal Astroglia. *Journal of Neuroscience*. 2007;27(32):8654–8664. doi:10.1523/JNEUROSCI.1615-07.2007.

12. Niu W, Zang T, Zou Y, et al. In vivo reprogramming of astrocytes to neuroblasts in the adult brain. *Nat Cell Biol*. 2013;15(10):1164–1175. doi:10.1038/ncb2843.

13. Torper O, Pfisterer U, Wolf DA, et al. Generation of induced neurons via direct conversion in vivo. *Proceedings of the National Academy of Sciences*. 2013;110(17):7038–7043. doi:10.1073/pnas.1303829110.

14. Oldham MC, Horvath S, Geschwind DH. Conservation and evolution of gene coexpression networks in human and chimpanzee brains. *Proceedings of the National Academy of Sciences*. 2006;103(47):17973–17978. doi:10.1073/pnas.0605938103.

15. Horvath S, Dong J. Geometric interpretation of gene coexpression network analysis. *PLoS Comput Biol*. 2008;4(8):e1000117. doi:10.1371/journal.pcbi.1000117.

16. Oldham MC, Konopka G, Iwamoto K, et al. Functional organization of the transcriptome in human brain. *Nat Neurosci*. 2008;11(11):1271–1282. doi:10.1038/nn.2207.

17. Langfelder P, Horvath S. WGCNA: an R package for weighted correlation network analysis. *BMC Bioinformatics*. 2008;9:559. doi:10.1186/1471-2105-9-559.

18. Scheffler B. Phenotypic and functional characterization of adult brain neuropoiesis. *Proceedings of the National Academy of Sciences*. 2005;102(26):9353–9358. doi:10.1073/pnas.0503965102.

19. Irizarry RA, Bolstad BM, Collin F, Cope LM, Hobbs B, Speed TP. Summaries of Affymetrix GeneChip probe level data. *Nucleic Acids Res*. 2003;31(4):e15.

20. Oldham MC, Langfelder P, Horvath S. Network methods for describing sample relationships in genomic datasets: application to Huntington's disease. *BMC Syst Biol*. 2012;6:63. doi:10.1186/1752-0509-6-63.

21. Bachoo RM, Kim RS, Ligon KL, et al. Molecular diversity of astrocytes with implications for neurological disorders. *Proc Natl Acad Sci USA*. 2004;101(22):8384–8389. doi:10.1073/pnas.0402140101.

22. Nielsen JA, Maric D, Lau P, Barker JL, Hudson LD. Identification of a novel oligodendrocyte cell adhesion protein using gene expression profiling. *Journal of Neuroscience*. 2006;26(39):9881–9891. doi:10.1523/JNEUROSCI.2246-06.2006.

23. Cahoy JD, Emery B, Kaushal A, et al. A transcriptome database for astrocytes, neurons, and oligodendrocytes: a new resource for understanding brain development and function. *Journal of Neuroscience*. 2008;28(1):264–278. doi:10.1523/JNEUROSCI.4178-07.2008.

24. Doyle JP, Dougherty JD, Heiman M, et al. Application of a translational profiling approach for the comparative analysis of CNS cell types. *Cell*. 2008;135(4):749–762. doi:10.1016/j.cell.2008.10.029.

25. Hamill OP, Marty A, Neher E, Sakmann B, Sigworth FJ. Improved patch-clamp techniques for high-resolution current recording from cells and cell-free membrane patches. *Pflugers Arch*. 1981;391(2):85–100.

26. Lim DA, Huang Y-C, Alvarez-Buylla A. Adult Subventricular Zone and Olfactory Bulb Neurogenesis. In: Gage FH, Kempermann G, Song H, eds. *Adult Neurogenesis*. Cold Spring Harbor Laboratory Press; 2008:175–206.

27. Ming G-L, Song H. Adult neurogenesis in the mammalian brain: significant answers and significant questions. *Neuron*. 2011;70(4):687–702. doi:10.1016/j.neuron.2011.05.001.

28. Benner EJ, Luciano D, Jo R, et al. Protective astrogenesis from the SVZ niche after injury is controlled by Notch modulator Thbs4. *Nature*. 2013;497(7449):369–373. doi:10.1038/nature12069.

29. Menn B. Origin of Oligodendrocytes in the Subventricular Zone of the Adult Brain. *Journal of Neuroscience*. 2006;26(30):7907–7918. doi:10.1523/JNEUROSCI.1299-06.2006.

30. Picard-Riera N, Decker L, Delarasse C, et al. Experimental autoimmune encephalomyelitis mobilizes neural progenitors from the subventricular zone to undergo oligodendrogenesis in adult mice. *Proc Natl Acad Sci USA*. 2002;99(20):13211–13216. doi:10.1073/pnas.192314199.

31. Nait-Oumesmar B, Decker L, Lachapelle F, Avellana-Adalid V, Bachelin C, Baron-Van Evercooren A. Progenitor cells of the adult mouse subventricular zone proliferate, migrate and differentiate into oligodendrocytes after demyelination. *Eur J Neurosci*. 1999;11(12):4357–4366.

32. Merkle FT, Mirzadeh Z, alvarez-Buylla A. Mosaic Organization of Neural Stem Cells in the Adult Brain. *Science*. 2007;317(5836):381–384. doi:10.1126/science.1144914.

33. Long JE, Garel S, Álvarez-Dolado M, et al. Dlx-dependent and -independent regulation of olfactory bulb interneuron differentiation. *Journal of Neuroscience*. 2007;27(12):3230–3243. doi:10.1523/JNEUROSCI.5265-06.2007.

34. Allen ZJ, Waclaw RR, Colbert MC, Campbell K. Molecular identity of olfactory bulb interneurons: transcriptional codes of periglomerular neuron subtypes. *J Mol Histol*. 2007;38(6):517–525. doi:10.1007/s10735-007-9115-4.

35. Panganiban G, Rubenstein JLR. Developmental functions of the Distal-less/Dlx homeobox genes. *Development*. 2002;129(19):4371–4386.

36. Colasante G, Collombat P, Raimondi V, et al. Arx is a direct target of Dlx2 and thereby contributes to the tangential migration of GABAergic interneurons.

Journal of Neuroscience. 2008;28(42):10674–10686. doi:10.1523/JNEUROSCI.1283-08.2008.

37. Shi Y, Chichung Lie D, Taupin P, et al. Expression and function of orphan nuclear receptor TLX in adult neural stem cells. *Nature*. 2004;427(6969):78–83. doi:10.1038/nature02211.

38. Ninkovic J, Steiner-Mezzadri A, Jawerka M, et al. The BAF Complex Interacts with Pax6 in Adult Neural Progenitors to Establish a Neurogenic Cross-Regulatory Transcriptional Network. *Cell Stem Cell*. 2013. doi:10.1016/j.stem.2013.07.002.

39. Jones WD, Dafou D, McEntagart M, et al. De novo mutations in MLL cause Wiedemann-Steiner syndrome. *Am J Hum Genet*. 2012;91(2):358–364. doi:10.1016/j.ajhg.2012.06.008.

40. Liu H-K, Wang Y, Belz T, et al. The nuclear receptor tailless induces long-term neural stem cell expansion and brain tumor initiation. *Genes & Development*. 2010;24(7):683–695. doi:10.1101/gad.560310.

41. Tian L, McClafferty H, Knaus HG, Ruth P, Shipston MJ. Distinct Acyl Protein Transferases and Thioesterases Control Surface Expression of Calcium-activated Potassium Channels. *Journal of Biological Chemistry*. 2012;287(18):14718–14725. doi:10.1074/jbc.M111.335547.

42. Saitoh F, Tian QB, Okano A, Sakagami H, Kondo H, Suzuki T. NIDD, a Novel DHHC-containing Protein, Targets Neuronal Nitric-oxide Synthase (nNOS) to the Synaptic Membrane through a PDZ-dependent Interaction and Regulates nNOS Activity.

43. Phippard D, Lu L, Lee D, Saunders JC, Crenshaw EB. Targeted mutagenesis of the POU-domain gene Brn4/Pou3f4 causes developmental defects in the inner ear. *Journal of Neuroscience*. 1999;19(14):5980–5989.

44. Mathis JM, Simmons DM, He X, Swanson LW, Rosenfeld MG. Brain 4: a novel mammalian POU domain transcription factor exhibiting restricted brain-specific

expression. *EMBO J*. 1992;11(7):2551–2561.

45. Parras CM, Galli R, Britz O, et al. Mash1 specifies neurons and oligodendrocytes in the postnatal brain. *EMBO J*. 2004;23(22):4495–4505. doi:10.1038/sj.emboj.7600447.

46. Wapinski OL, Vierbuchen T, Qu K, et al. Hierarchical mechanisms for direct reprogramming of fibroblasts to neurons. *Cell*. 2013;155(3):621–635. doi:10.1016/j.cell.2013.09.028.

47. Takahashi K, Tanabe K, Ohnuki M, et al. Induction of Pluripotent Stem Cells from Adult Human Fibroblasts by Defined Factors. *Cell*. 2007;131(5):861–872. doi:10.1016/j.cell.2007.11.019.

48. Yu J, Vodyanik MA, Smuga-Otto K, et al. Induced Pluripotent Stem Cell Lines Derived from Human Somatic Cells. *Science*. 2007;318(5858):1917–1920. doi:10.1126/science.1151526.

49. Park I-H, Zhao R, West JA, et al. Reprogramming of human somatic cells to pluripotency with defined factors. *Nature*. 2008;451(7175):141–146. doi:doi:10.1038/nature06534.

50. Gonzales-Roybal G, Lim DA. Chromatin-based epigenetics of adult subventricular zone neural stem cells. *Front Genet*. 2013;4. doi:10.3389/fgene.2013.00194.

FIGURE LEGENDS

Figure 1. *Mll1* is required for neurogenesis but not for gliogenesis. A) Differentiation of wild-type SVZ NSCs over a 7-day time course. B) Differentiation of Mll1-deleted SVZ NSCs. Tuj1+ neurons are shown in panels i-iv while O4+ and NG2+ oligodendrocytes are shown in panels v and vi. Panels i-iv: GFAP (green), Tuj1 (red), DAPI (blue). Panels v and vi: O4 (green), and NG2 (red). Scale bar, 50μm. Panels Ai-iv were originally published in Gonzalez-Roybal and Lim.[50]

Figure 2. Gene coexpression analysis identifies distinct transcriptional modules. A) Hierarchical clustering of gene coexpression modules. This dendrogram was produced using average linkage hierarchical clustering with 1 – the Pearson correlation of the module eigengenes[15] (first principal components) as a distance measure. B-C) Select gene coexpression modules showing representative heatmaps and first principal components at 0 (self-renewal conditions), 1, 2, and 4 days of differentiation in wild-type (WT) and *Mll1*-deleted ($Mll1^{\Delta/\Delta}$) NSCs. B) Non-neurogenic modules identified through gene coexpression analysis. C) *Mll1*-dependent modules that are enriched for neurogenic gene expression. Lowercase letters in B and C indicate independent biological replicates.

Figure 3. Rescue of neurogenesis by overexpression of select transcription factors. A-F) Immunocytochemistry of *hGFAP-Cre;*$Mll1^{f/f}$ SVZ NSC cultures after 4 days of differentiation and enforced expression with lentiviral constructs containing select Mll1-dependent factors: control (A), *Dlx2* (B), *Brn4* (C), *Tlx* (D), *Zdhhc23* (E) and *Shisa3* (F). GFP (green), Tuj1 (red), DAPI (blue). G) Quantification of infected (GFP+) cells that are also Tuj1+ (n=3 wells). Error bars = standard deviation. One-way ANOVA with post-hoc Dunnett's test was used to compare each experimental factor to *hPLAP* control. Scale bar, 50μm.

Figure 4. Brn4 induces neurogenesis in cortically-derived astroglia. Immunocytochemistry of cortically-derived astroglial cultures before (A) and 20 days after (B-F) neuronal differentiation and enforced lentiviral expression of *Brn4*. B-F) Examples of cells with neuronal morphology expressing various neuronal markers: Tuj1

(B), MAP2 (C), DCX (D), GAD67 (E), and CalB (F). GFAP (red, A), DAPI (blue, A-F); GFP (green, B-F). No cells with neuronal morphology expressing these neuronal markers were identified in control-infected cultures. G) Quantification of infected (GFP+) cells that were also Tuj1+, MAP2+, or DCX+ (from B, C, and D, respectively; compared to *hPLAP* controls; n=3 wells for each). Error bars = standard deviation. Student's t-test used to compare Brn4 to *hPLAP* for each stain. Scale bars: A) 50μm; B-F) 25μm.

Figure 5. Electrophysiologic analysis of neurons induced by Brn4 overexpression in cortically-derived astroglia. A) Phase contrast image of a sample recorded neuron. B) Action potentials were elicited by a series of current injections ranging from -40 to +80 pA in 20 pA increments. Action potentials were reversibly blocked with 1 μM TTX.

Supplementary Figure 1. Transcriptional modules identified through gene coexpression analysis. Gene coexpression analysis was performed on microarray data from wild-type and *Mll1*-deleted SVZ NSC cultures at 0 (self-renewal conditions), 1, 2, and 4 days after differentiation. Fourteen transcriptional modules were identified and labeled by colors (A-N). Each page shows a snapshot for a given module consisting of a heat map, a barplot of the module eigengene (ME, or first principal component), and the top 15 genes based on the strength of module membership (kME). Where microarray probes did not correspond to a known gene "*NA*" is listed as the gene name. The presence of a given gene more than once in the top genes by kME indicates that there were multiple microarray probes corresponding to that gene. All samples were analyzed in biological triplicates.

Figure 1
Click here to download high resolution image

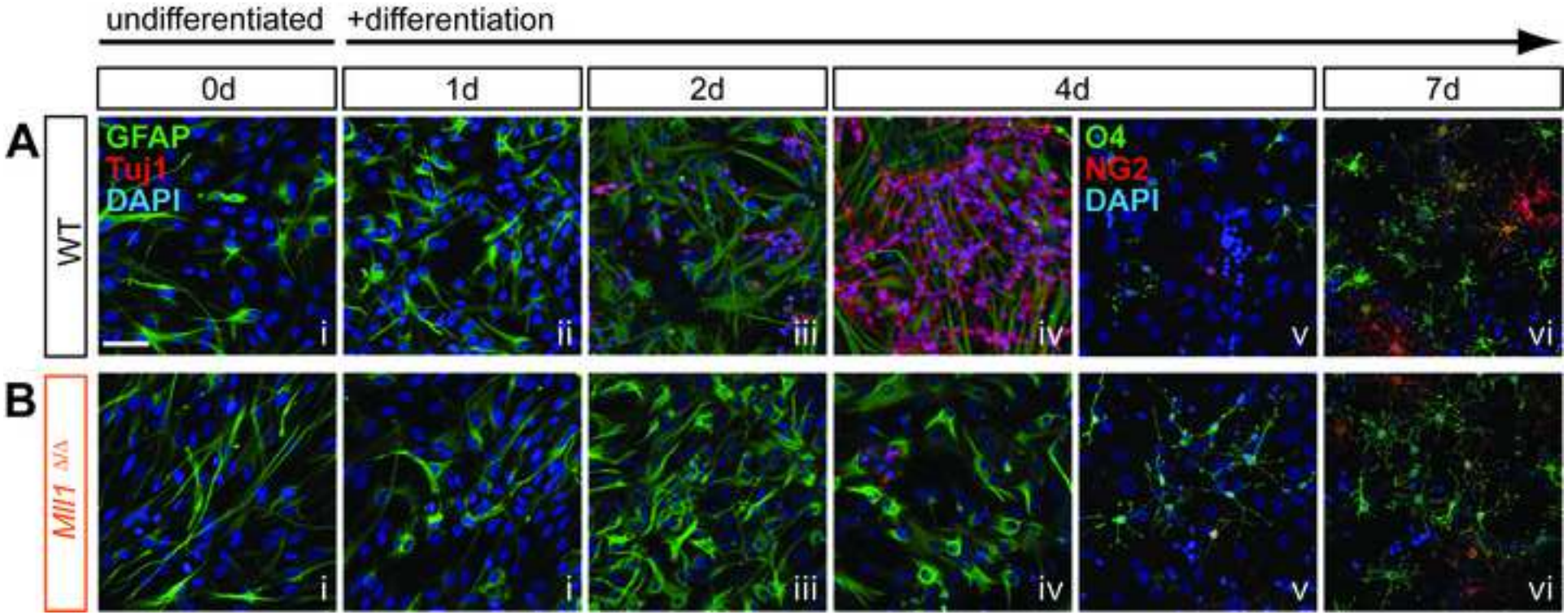

Figure 2
Click here to download high resolution image

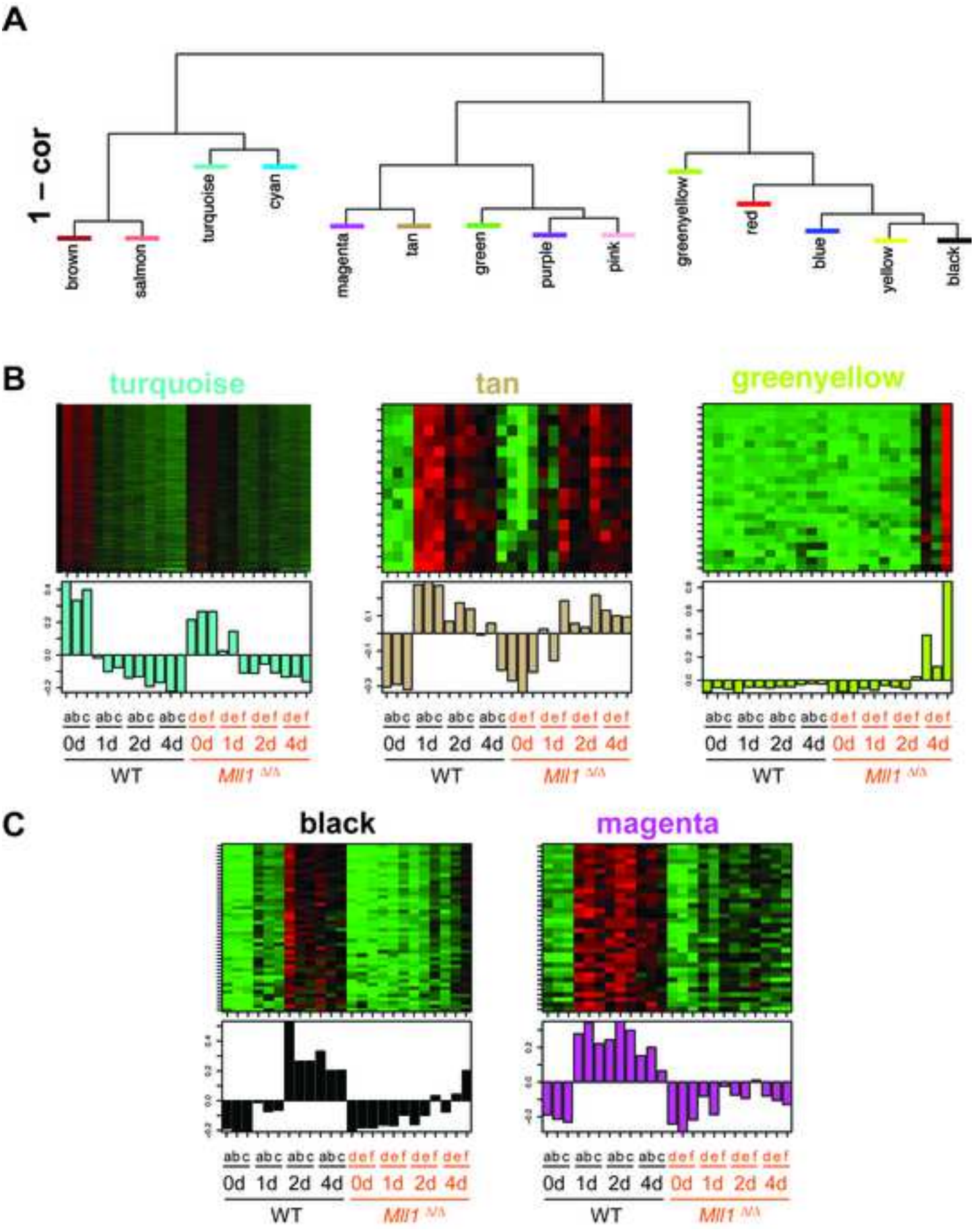

Figure 3
Click here to download high resolution image

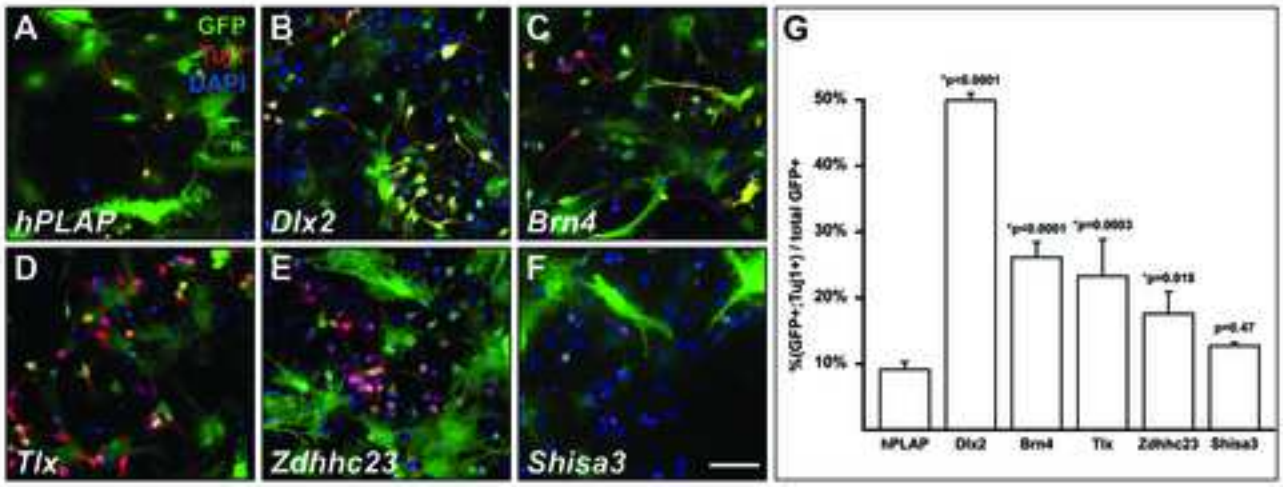

Figure 4
Click here to download high resolution image

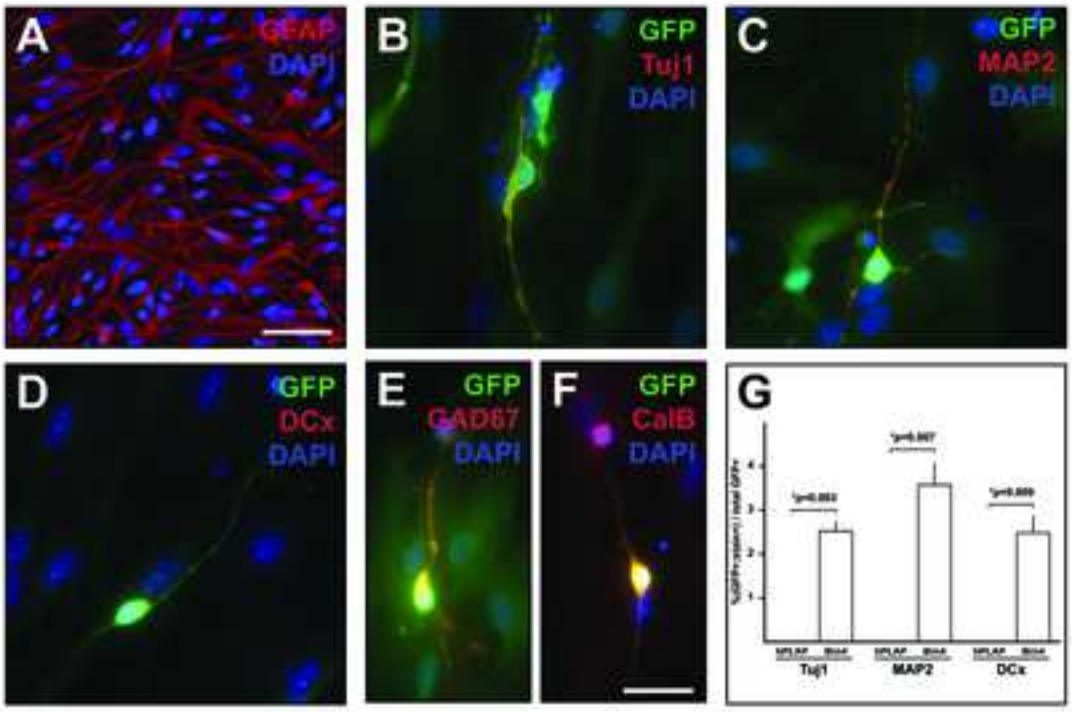

Figure 5
Click here to download high resolution image

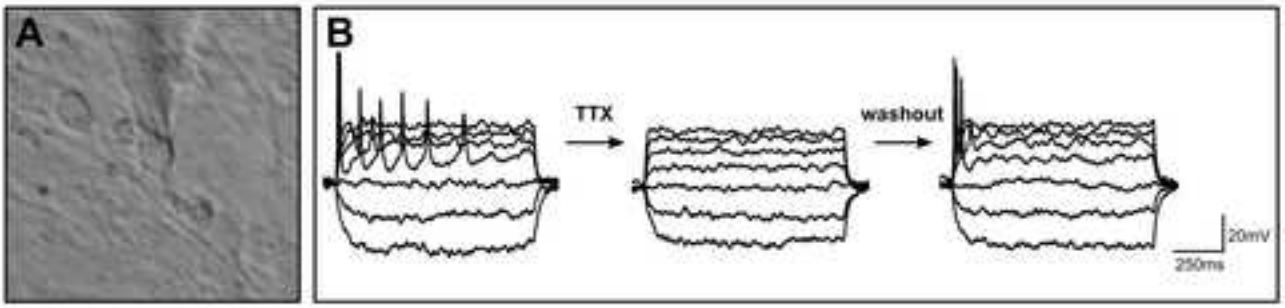

Table 1. Gene ontology terms associated with select transcriptional modules

Module	Top five gene ontology (GO) terms	p-value
Turquoise	GO:0007049~cell cycle	6.44E-42
	GO:0022402~cell cycle process	9.04E-39
	GO:0022403~cell cycle phase	1.95E-37
	GO:0000279~M phase	1.51E-34
	GO:0000278~mitotic cell cycle	2.93E-33
Tan	GO:0019725~cellular homeostasis	4.51E-03
	GO:0019228~regulation of action potential in neuron	4.76E-03
	GO:0010975~regulation of neuron projection development	5.39E-03
	GO:0019226~transmission of nerve impulse	7.43E-03
	GO:0001508~regulation of action potential	7.93E-03
Greenyellow	GO:0007272~ensheathment of neurons	1.09E-06
	GO:0008366~axon ensheathment	1.09E-06
	GO:0019228~regulation of action potential in neuron	1.96E-06
	GO:0001508~regulation of action potential	4.11E-06
	GO:0048709~oligodendrocyte differentiation	7.26E-06
Black	GO:0031175~neuron projection development	1.97E-06
	GO:0048666~neuron development	4.01E-06
	GO:0030182~neuron differentiation	1.36E-05
	GO:0030030~cell projection organization	5.68E-05
	GO:0007409~axonogenesis	1.13E-04
Magenta	GO:0030900~forebrain development	1.35E-03
	GO:0021537~telencephalon development	1.93E-03
	GO:0021879~forebrain neuron differentiation	4.60E-03
	GO:0006928~cell motion	5.25E-03
	GO:0021872~generation of neurons in the forebrain	6.01E-03

Table 2. Lentiviral expression vectors

Magenta module genes (neurogenic)
LV-*Dlx2*-GFP
LV-*Brn4*-GFP
LV-*Tlx*-GFP
LV-*Zdhhc23*-GFP
Mll1-independent gene (non-neurogenic)
LV-*Shisa3*-GFP
Control vector
LV-*hPLAP*-GFP

Supplemental Figure 1A

Click here to download Supplemental Content (for online-only posting): Suppl Figure 1A.eps

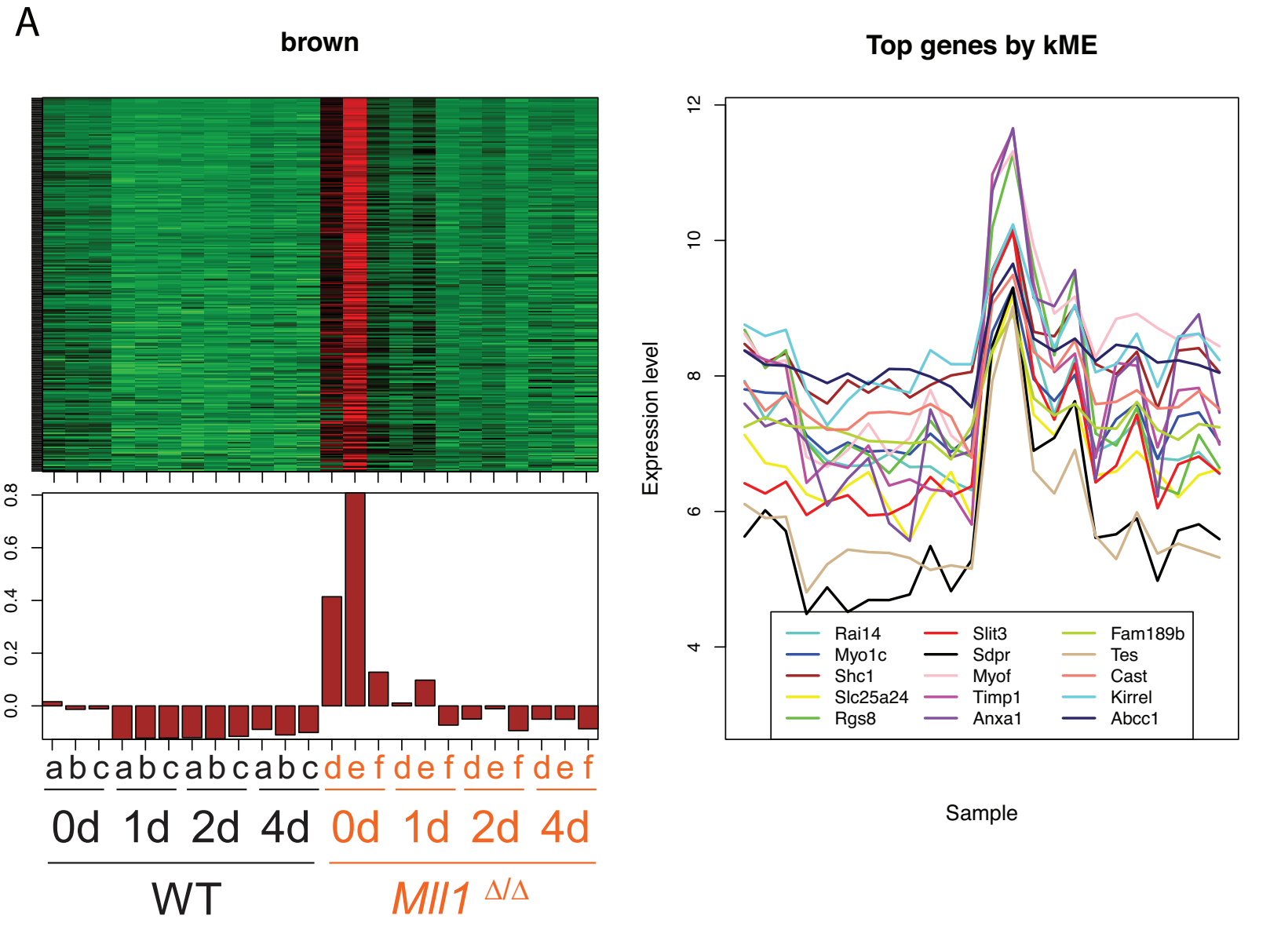

Supplemental Figure 1B

Click here to download Supplemental Content (for online-only posting): Suppl Figure 1B.eps

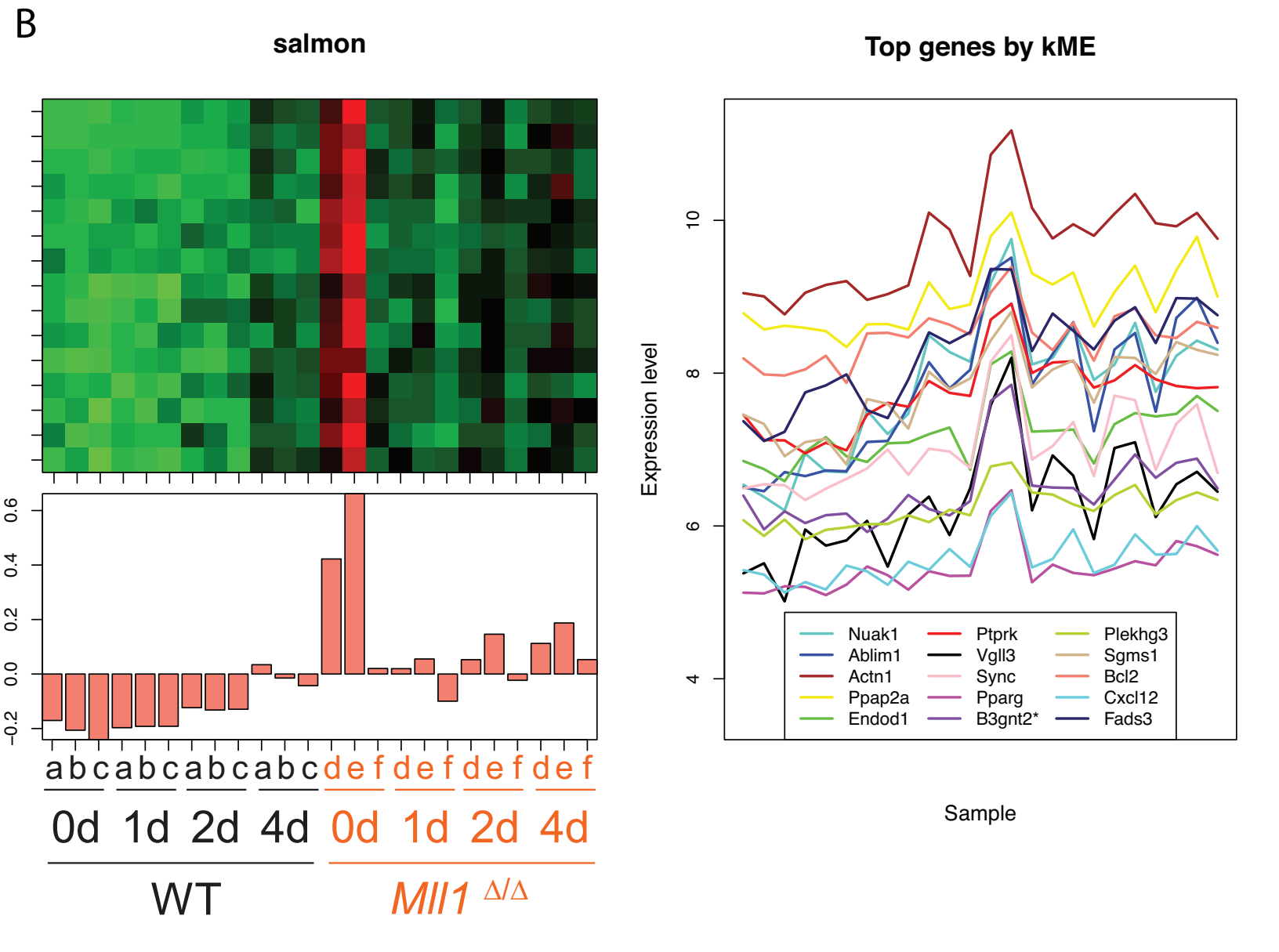

Supplemental Figure 1C

Click here to download Supplemental Content (for online-only posting): Suppl Figure 1C.eps

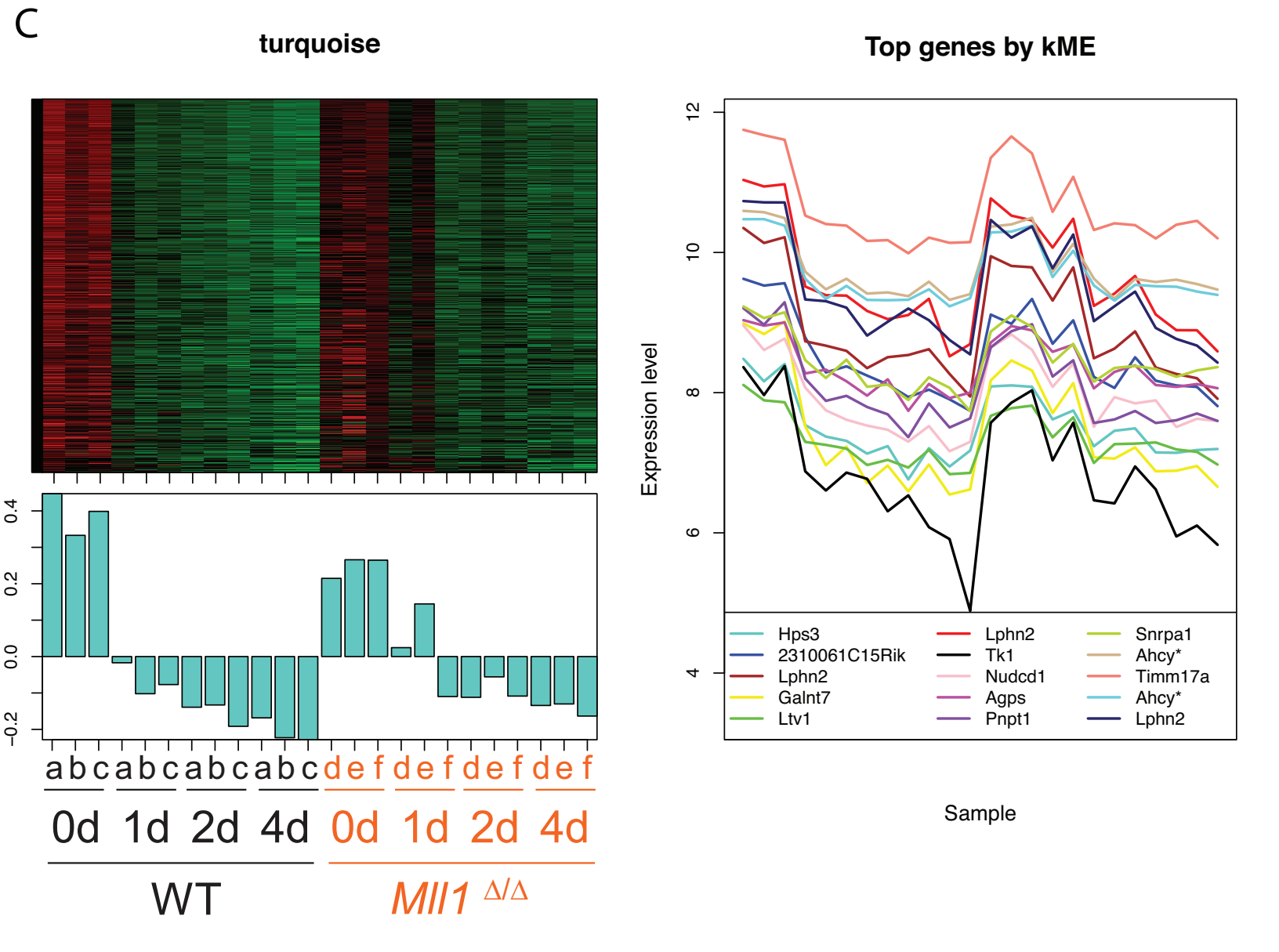

Supplemental Figure 1D

Click here to download Supplemental Content (for online-only posting): Suppl Figure 1D.eps

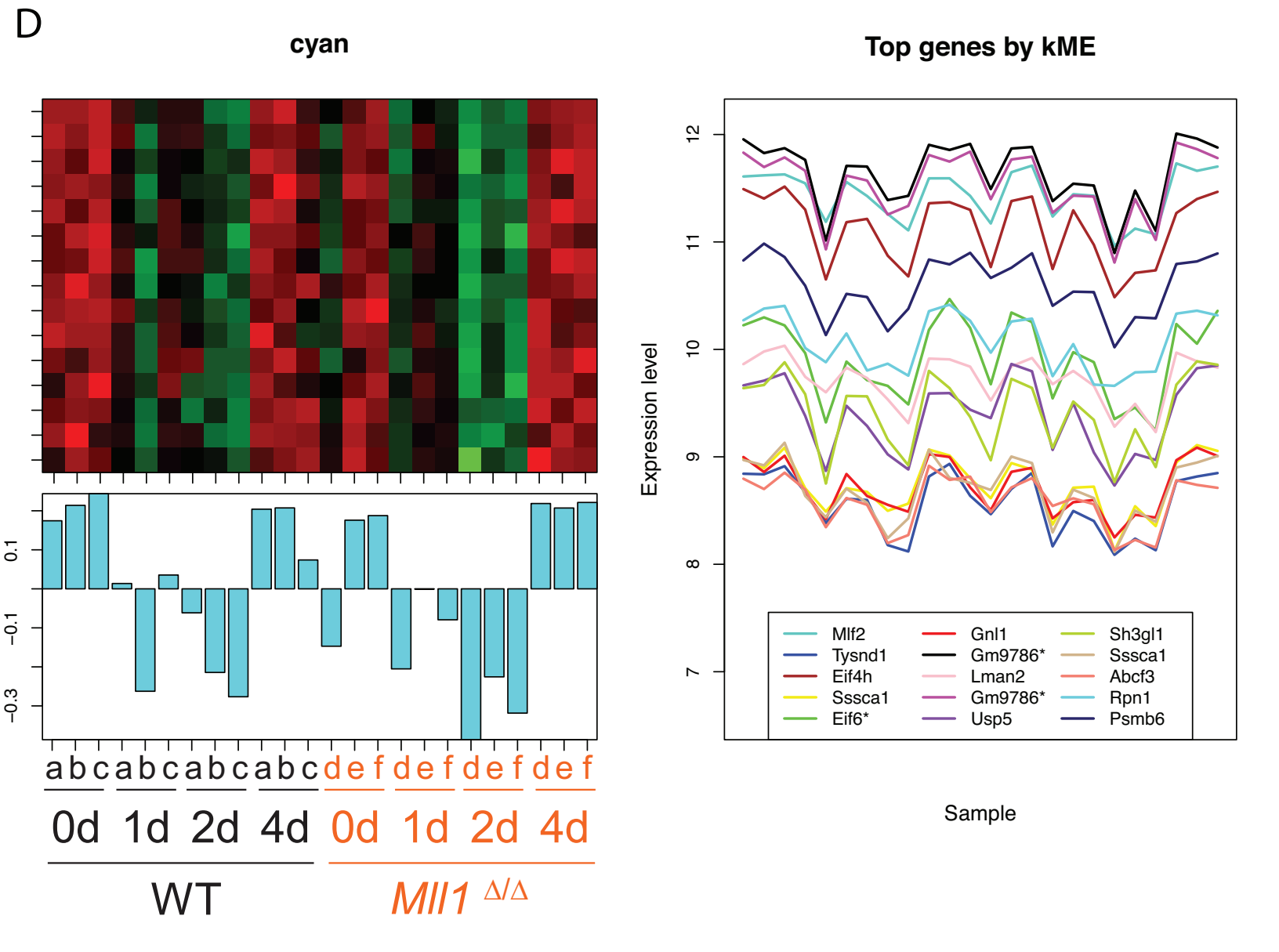

Supplemental Figure 1E

Click here to download Supplemental Content (for online-only posting): Suppl Figure 1E.eps

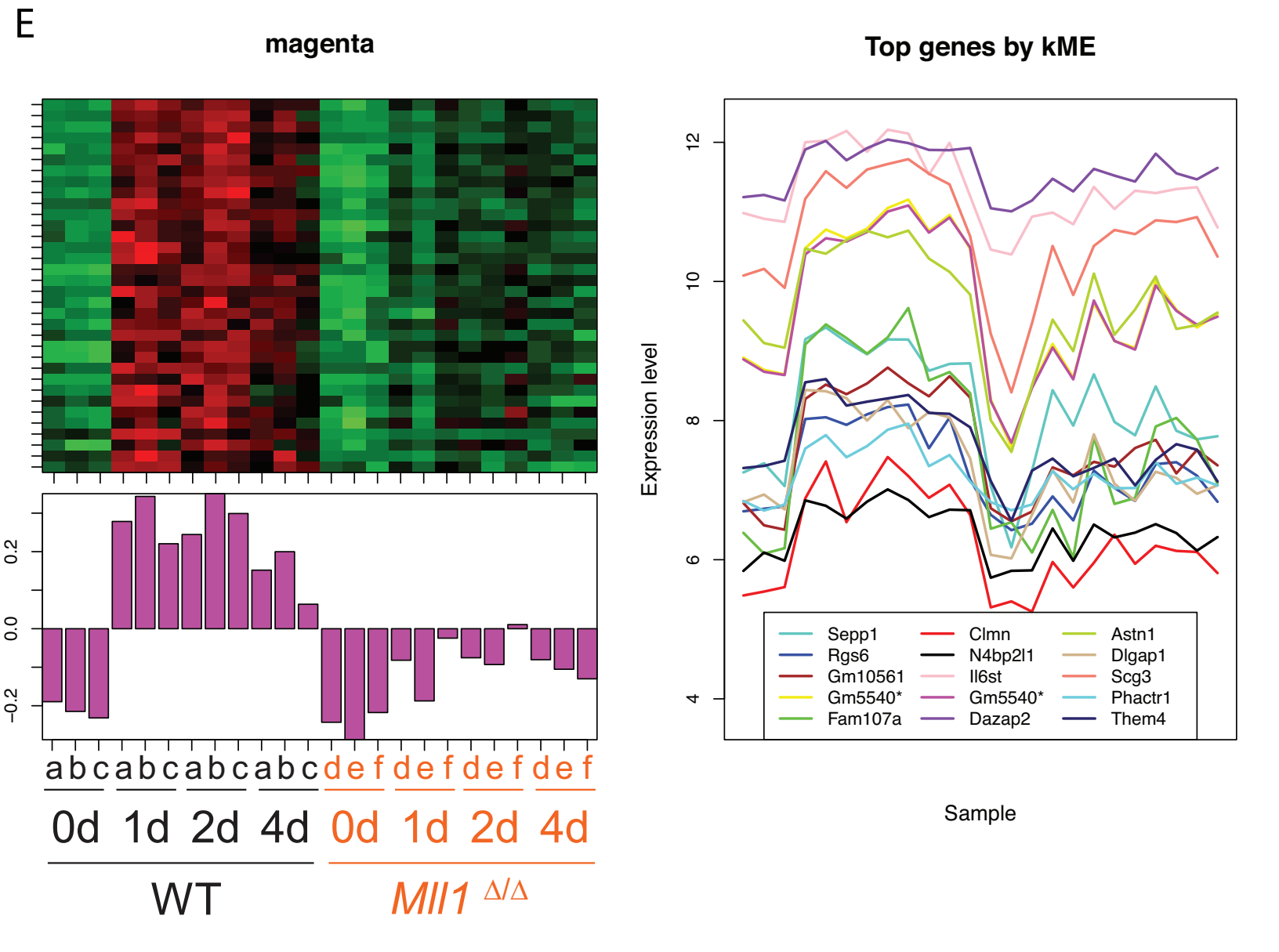

Supplemental Figure 1F

Click here to download Supplemental Content (for online-only posting): Suppl Figure 1F.eps

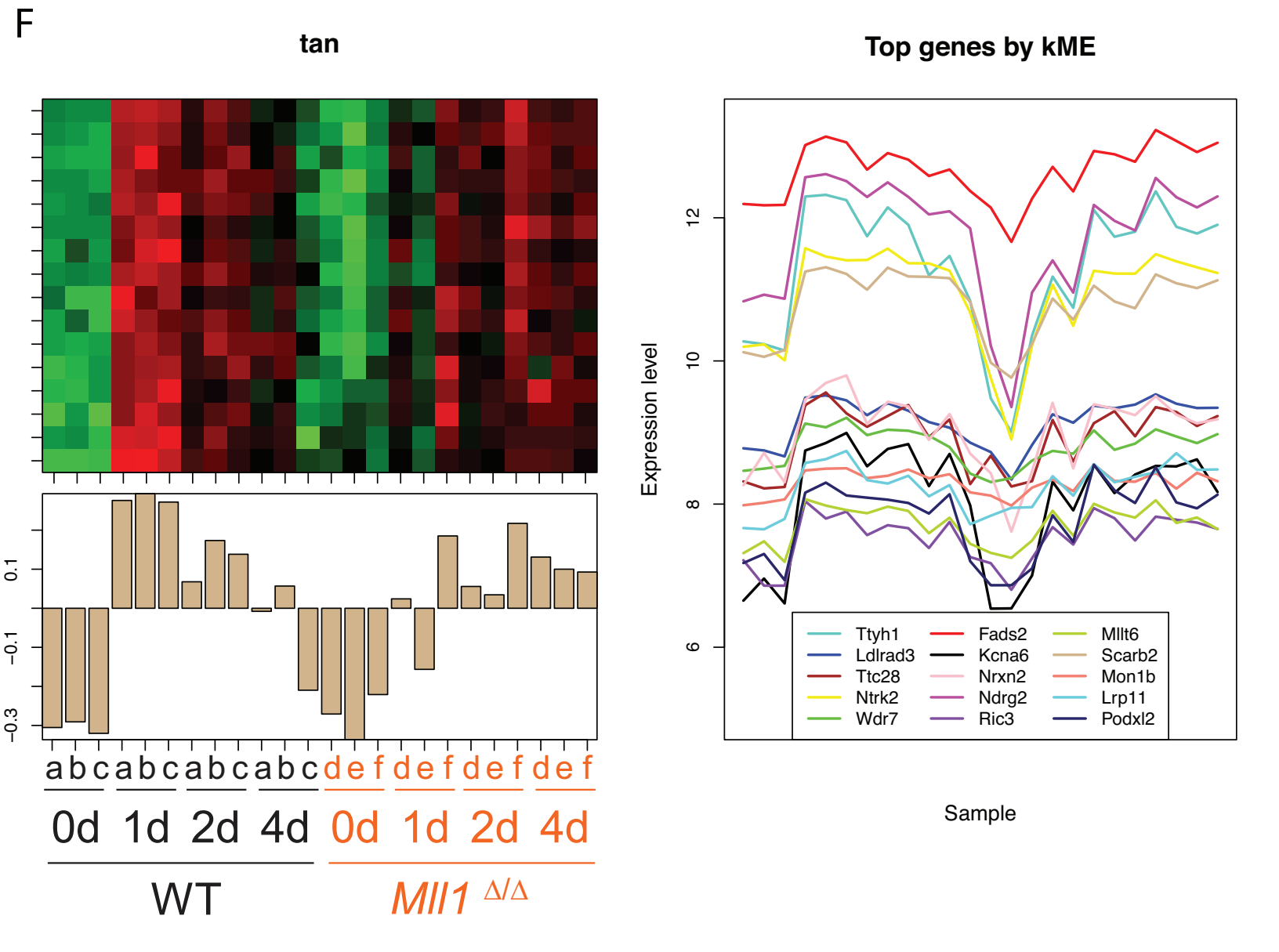

Supplemental Figure 1G

Click here to download Supplemental Content (for online-only posting): Suppl Figure 1G.eps

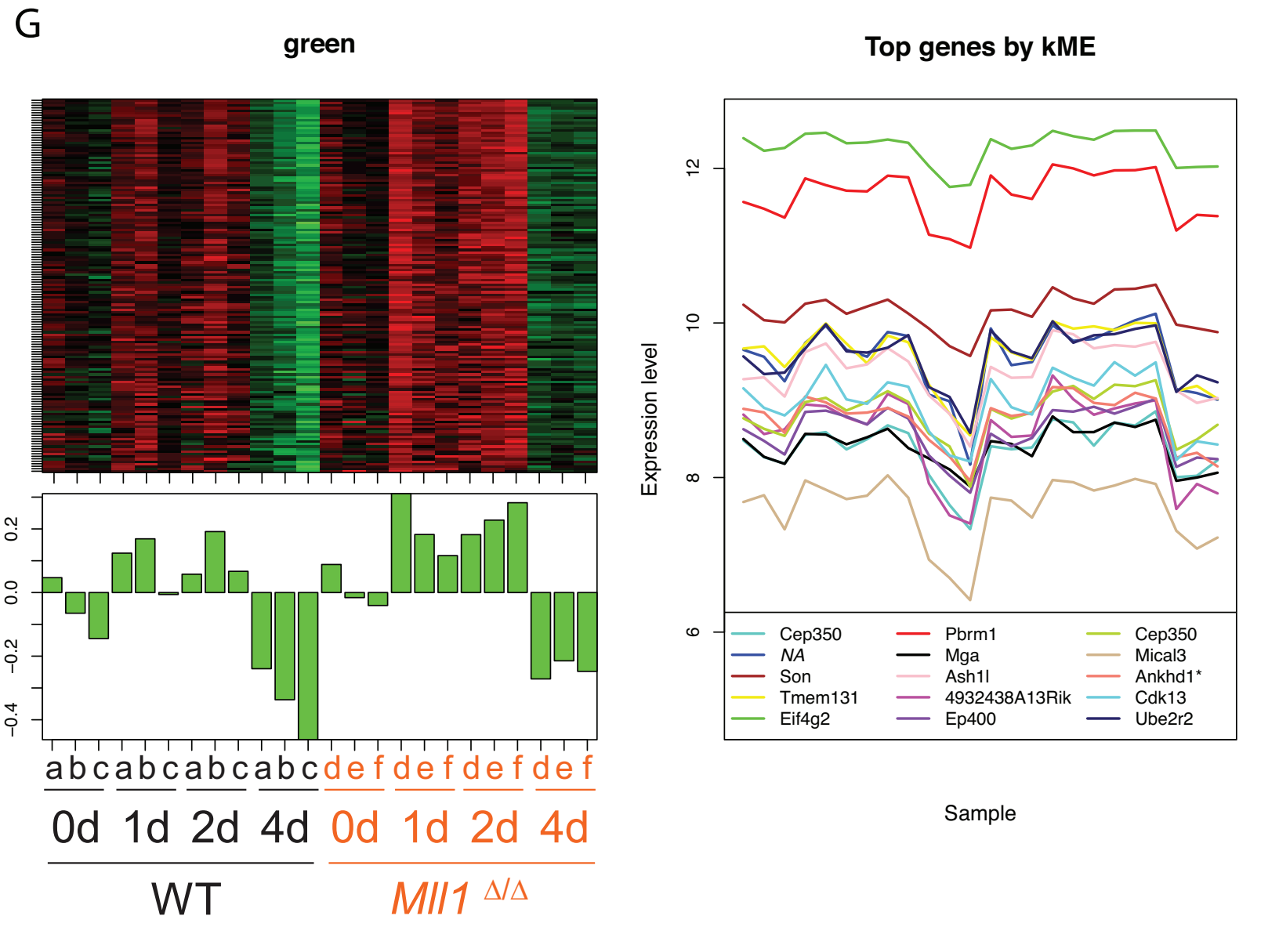

Supplemental Figure 1H

Click here to download Supplemental Content (for online-only posting): Suppl Figure 1H.eps

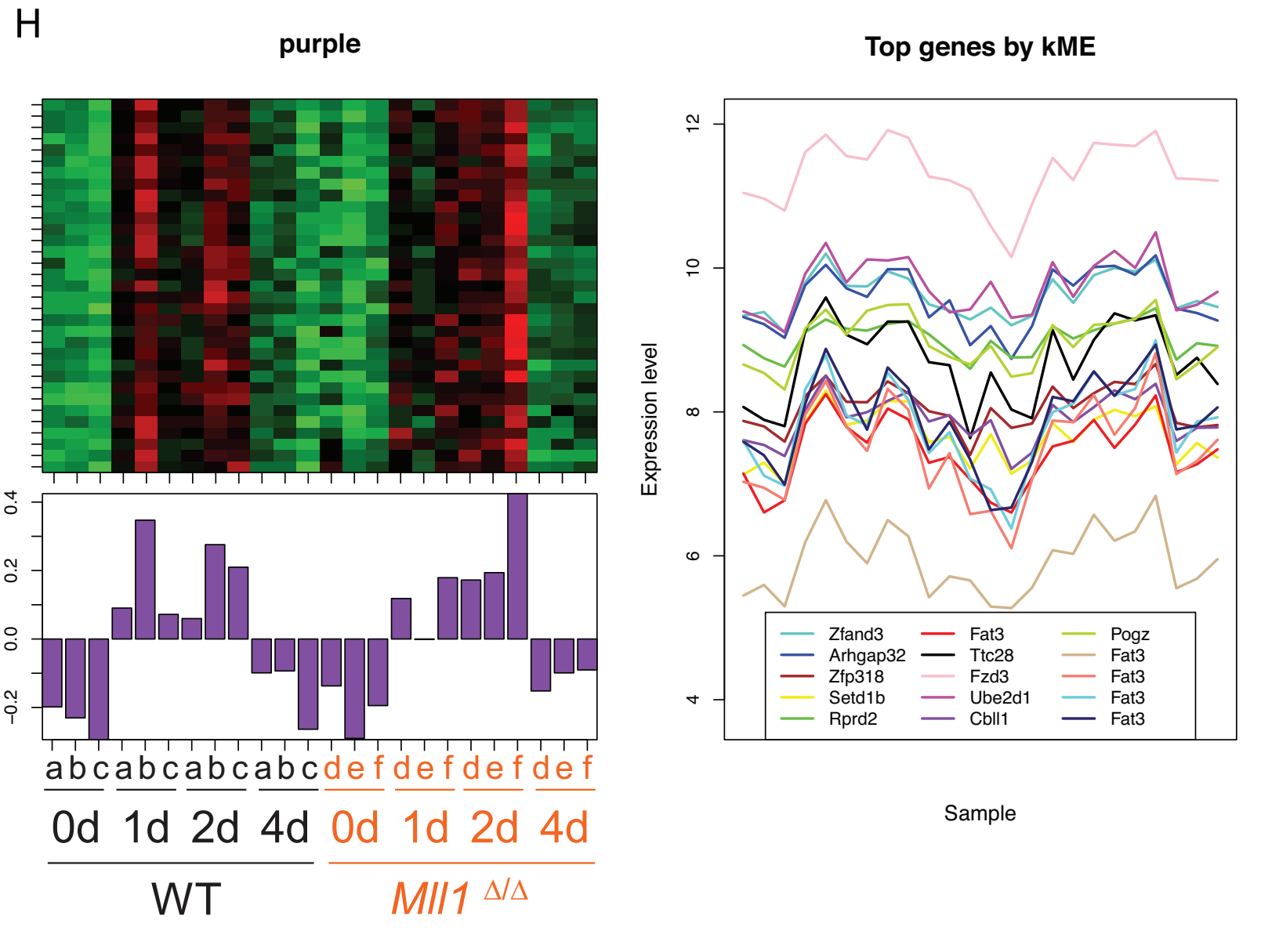

Supplemental Figure 1I

Click here to download Supplemental Content (for online-only posting): Suppl Figure 1I.eps

I

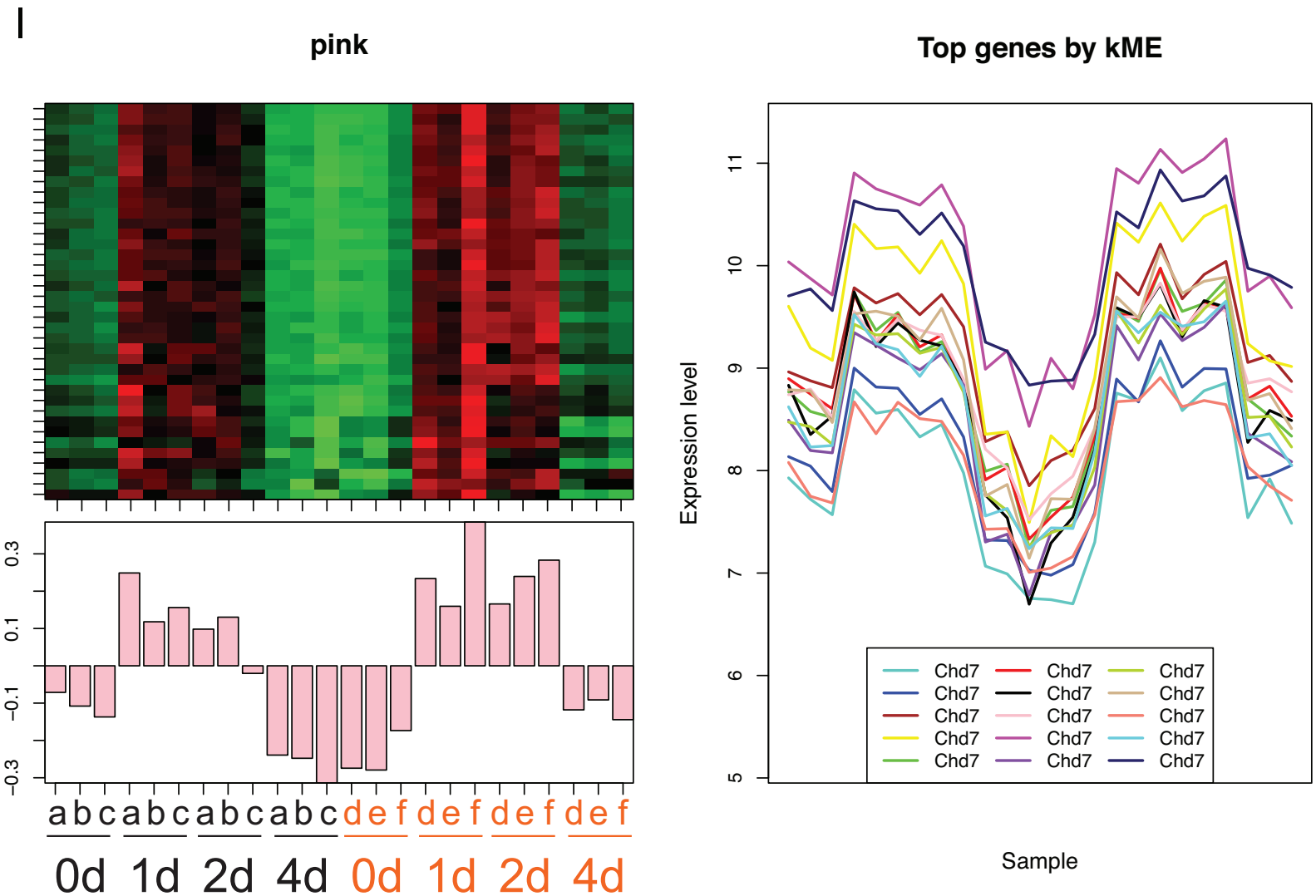

Supplemental Figure 1J

Click here to download Supplemental Content (for online-only posting): Suppl Figure 1J.eps

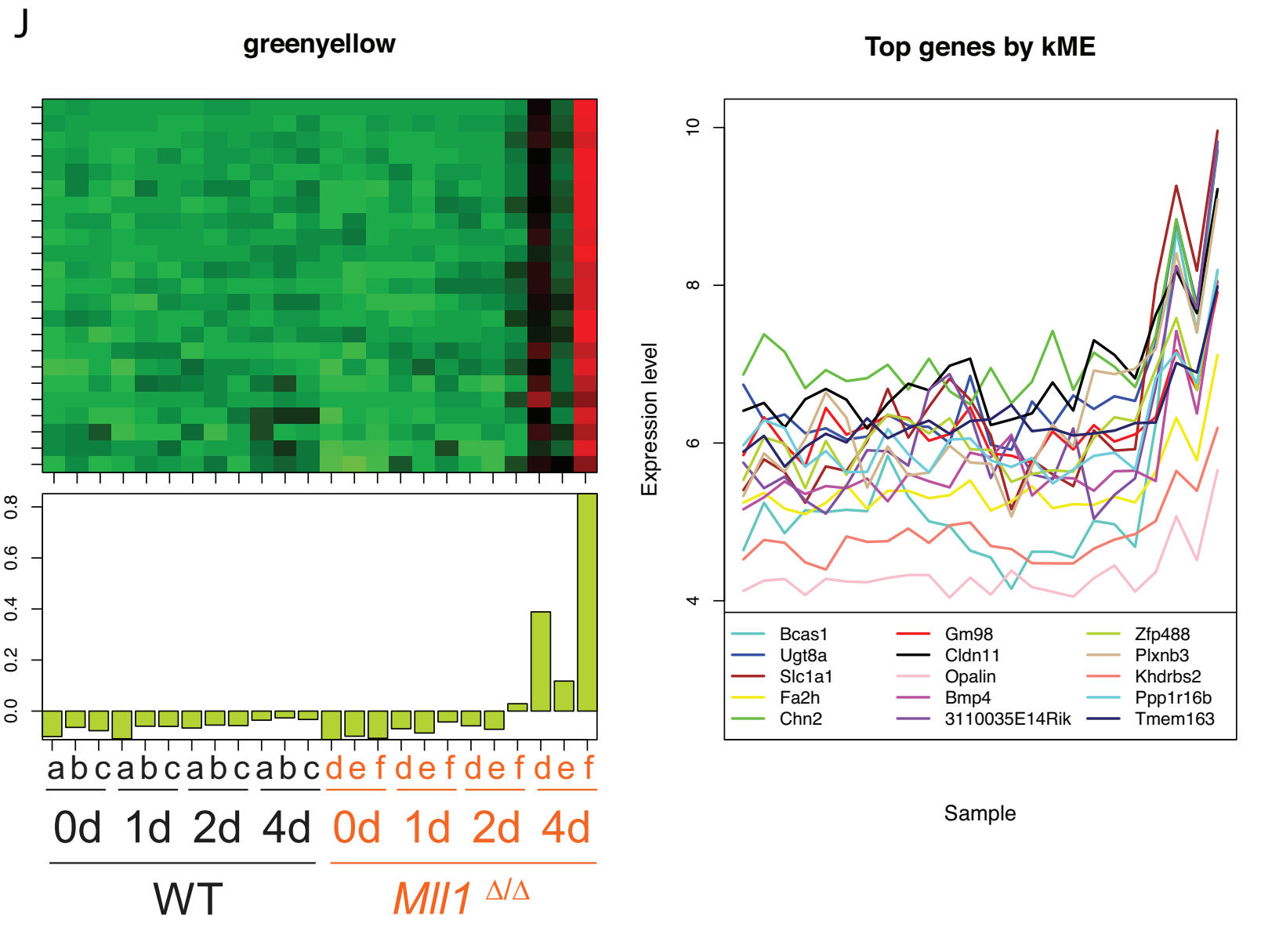

Supplemental Figure 1K

Click here to download Supplemental Content (for online-only posting): Suppl Figure 1K.eps

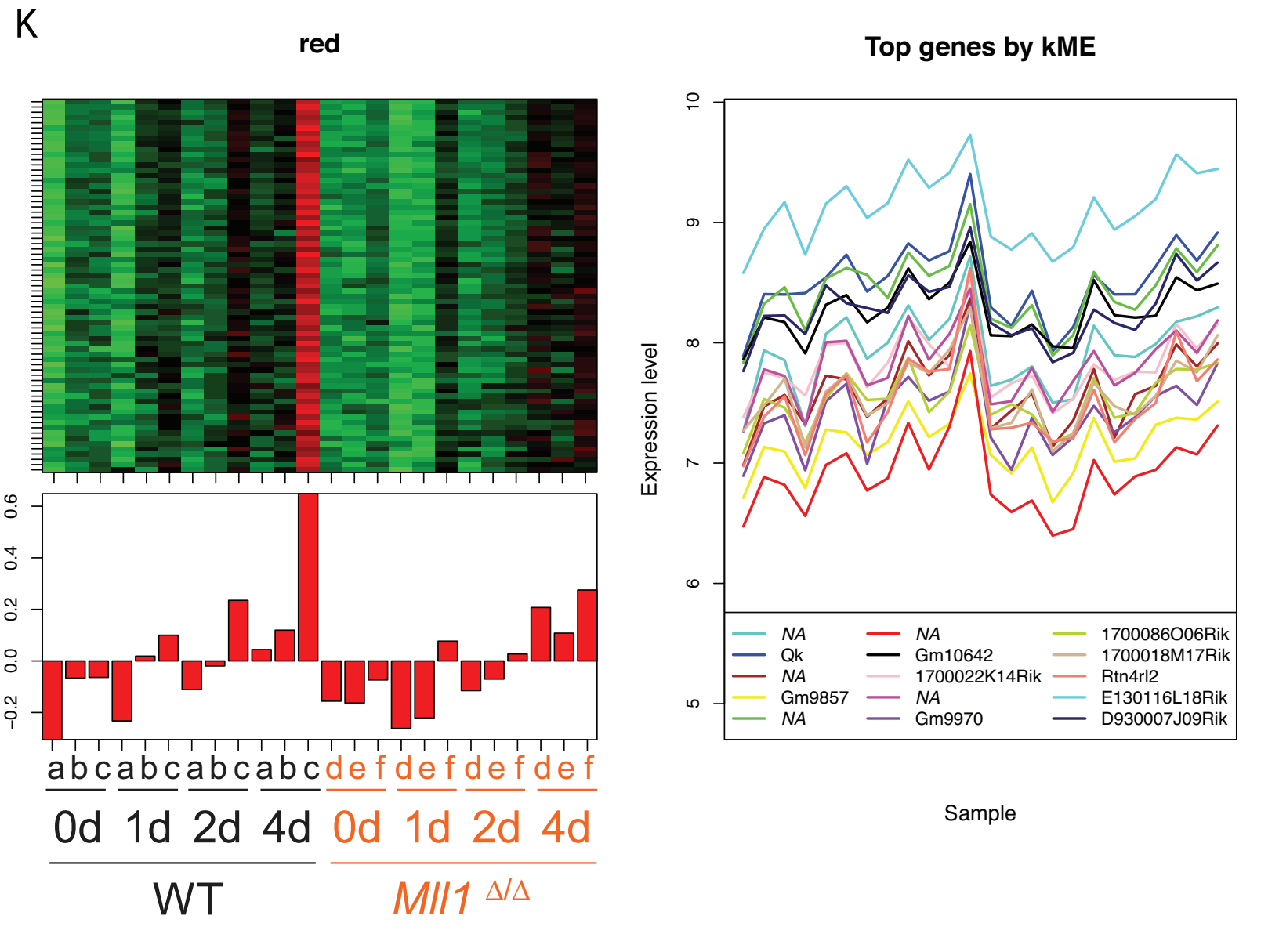

Supplemental Figure 1L

Click here to download Supplemental Content (for online-only posting): Suppl Figure 1L.eps

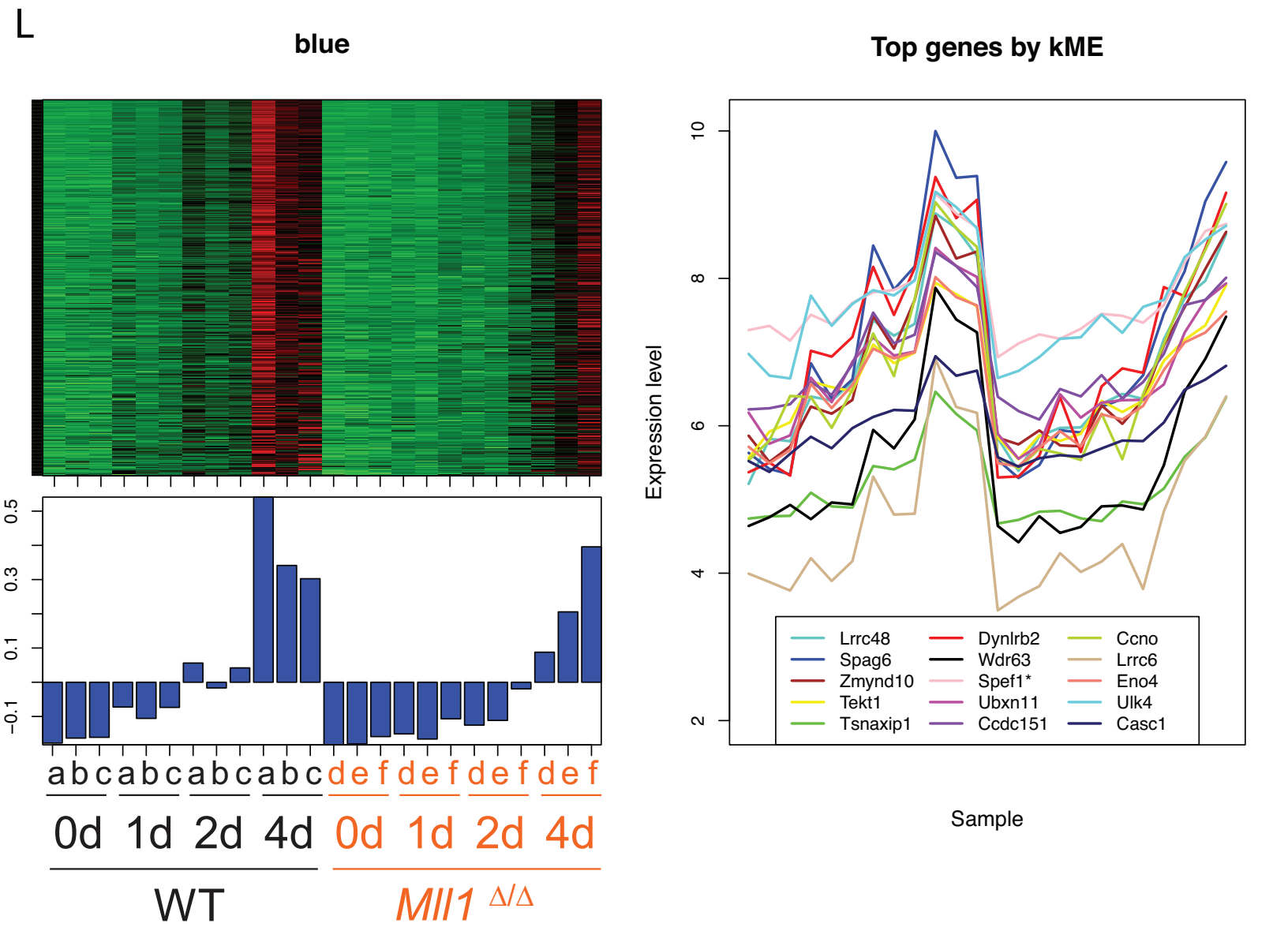

Supplemental Figure 1M

Click here to download Supplemental Content (for online-only posting): Suppl Figure 1M.eps

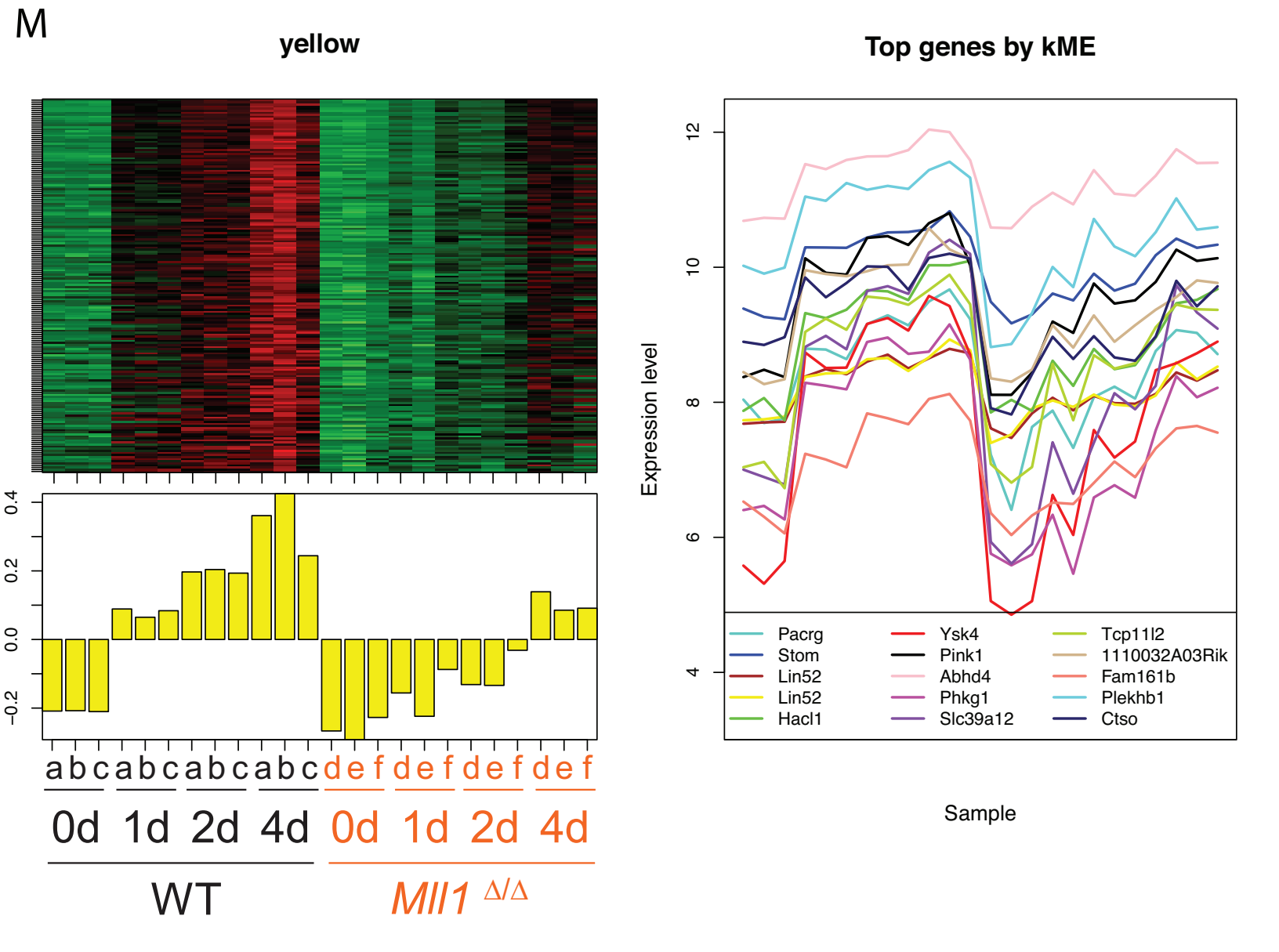

Supplemental Figure 1N

Click here to download Supplemental Content (for online-only posting): Suppl Figure 1N.eps

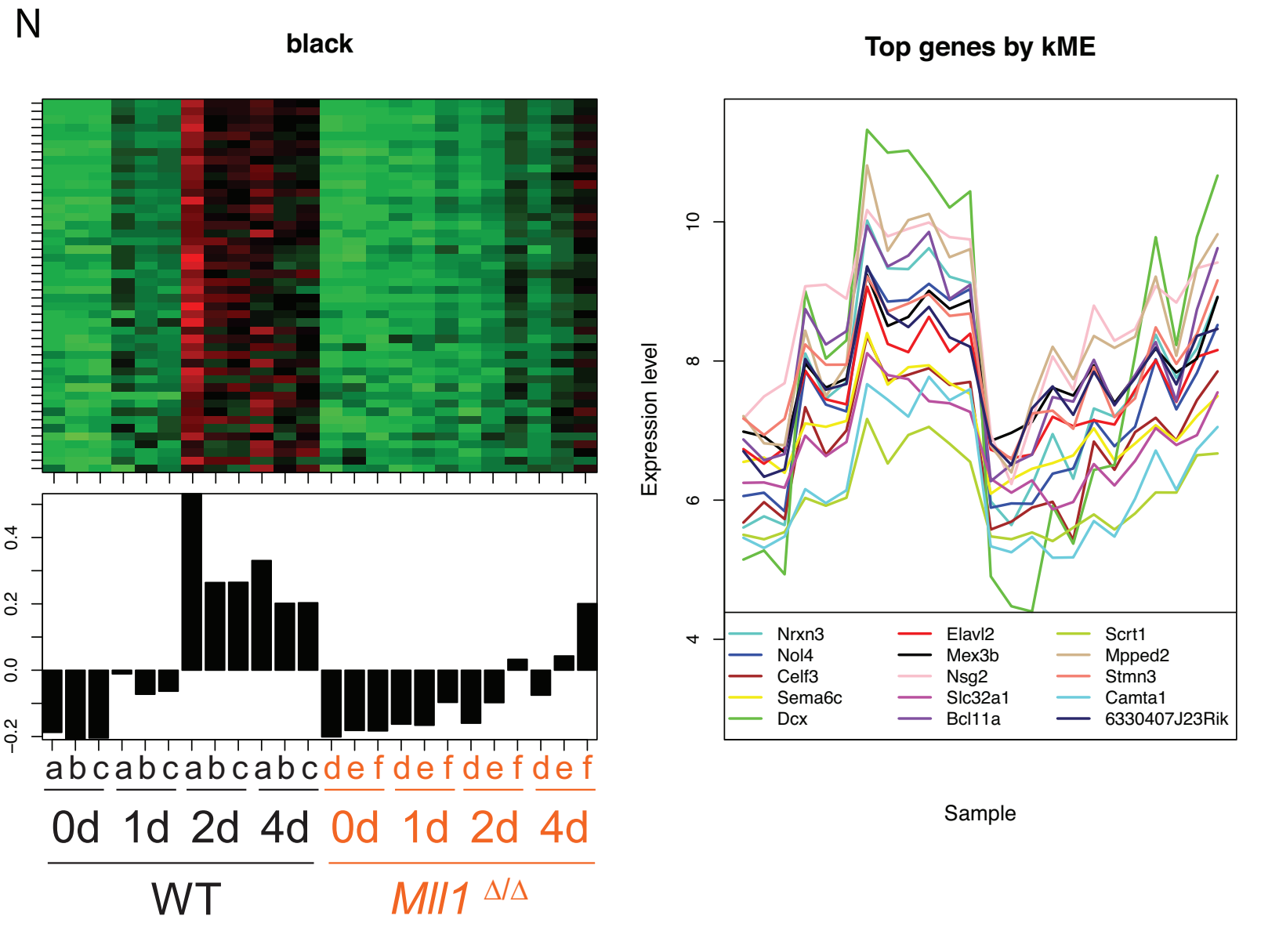

Supplemental Table 1
Click here to download Supplemental Content (for online-only posting): Brn4 Supp Table1 2014-04-12.docx

Supplementary Table 1. Gene ontology terms associated with *Mll1*-dependent and -independent transcriptional modules

Module	Top five gene ontology (GO) terms	p-value
	***Mll1*-dependent**	
Black	GO:0031175~neuron projection development	1.97E-06
	GO:0048666~neuron development	4.01E-06
	GO:0030182~neuron differentiation	1.36E-05
	GO:0030030~cell projection organization	5.68E-05
	GO:0007409~axonogenesis	1.13E-04
Blue	GO:0007017~microtubule-based process	2.04E-09
	GO:0007018~microtubule-based movement	2.34E-09
	GO:0030030~cell projection organization	4.90E-06
	GO:0060271~cilium morphogenesis	3.52E-05
	GO:0030031~cell projection assembly	3.82E-03
Brown	GO:0048514~blood vessel morphogenesis	8.80E-08
	GO:0001568~blood vessel development	1.20E-07
	GO:0001944~vasculature development	1.81E-07
	GO:0001525~angiogenesis	2.56E-07
	GO:0016477~cell migration	1.62E-06
Greenyellow	GO:0007272~ensheathment of neurons	1.09E-06
	GO:0008366~axon ensheathment	1.09E-06
	GO:0019228~regulation of action potential in neuron	1.96E-06
	GO:0001508~regulation of action potential	4.11E-06
	GO:0048709~oligodendrocyte differentiation	7.26E-06
Magenta	GO:0030900~forebrain development	1.35E-03
	GO:0021537~telencephalon development	1.93E-03
	GO:0021879~forebrain neuron differentiation	4.60E-03
	GO:0006928~cell motion	5.25E-03
	GO:0021872~generation of neurons in the forebrain	6.01E-03
Salmon	GO:0030334~regulation of cell migration	2.57E-05
	GO:0051094~positive regulation of developmental process	5.97E-05
	GO:0051270~regulation of cell motion	6.03E-05
	GO:0040012~regulation of locomotion	7.04E-05
	GO:0030030~cell projection organization	1.77E-04
Yellow	GO:0006412~translation	5.91E-05
	GO:0007018~microtubule-based movement	4.34E-04
	GO:0051301~cell division	9.29E-04
	GO:0007049~cell cycle	9.35E-04
	GO:0030258~lipid modification	1.85E-03

Module	Top five gene ontology (GO) terms	p-value
	***Mll*-independent**	
Cyan	GO:0016573~histone acetylation	1.97E-07
	GO:0006473~protein amino acid acetylation	2.35E-07
	GO:0043543~protein amino acid acylation	1.38E-06
	GO:0016570~histone modification	5.78E-05
	GO:0016569~covalent chromatin modification	7.36E-05
Green	GO:0016568~chromatin modification	1.55E-12
	GO:0006325~chromatin organization	2.97E-11
	GO:0051276~chromosome organization	8.56E-11
	GO:0045449~regulation of transcription	8.58E-09
	GO:0006350~transcription	1.06E-07
Pink	GO:0045449~regulation of transcription	1.40E-06
	GO:0006357~regulation of transcription from RNA polymerase II promoter	3.72E-06
	GO:0006355~regulation of transcription, DNA-dependent	1.32E-04
	GO:0051252~regulation of RNA metabolic process	1.57E-04
	GO:0006350~transcription	3.37E-04
Purple	GO:0045449~regulation of transcription	1.38E-07
	GO:0030163~protein catabolic process	3.25E-07
	GO:0009057~macromolecule catabolic process	5.61E-07
	GO:0006325~chromatin organization	3.72E-06
	GO:0044265~cellular macromolecule catabolic process	5.52E-06
Red	GO:0006355~regulation of transcription, DNA-dependent	7.12E-08
	GO:0051252~regulation of RNA metabolic process	1.04E-07
	GO:0030182~neuron differentiation	4.10E-06
	GO:0045449~regulation of transcription	1.66E-05
	GO:0014706~striated muscle tissue development	8.17E-05
Tan	GO:0019725~cellular homeostasis	4.51E-03
	GO:0019228~regulation of action potential in neuron	4.76E-03
	GO:0010975~regulation of neuron projection development	5.39E-03
	GO:0019226~transmission of nerve impulse	7.43E-03
	GO:0001508~regulation of action potential	7.93E-03
Turquoise	GO:0007049~cell cycle	6.44E-42
	GO:0022402~cell cycle process	9.04E-39
	GO:0022403~cell cycle phase	1.95E-37
	GO:0000279~M phase	1.51E-34
	GO:0000278~mitotic cell cycle	2.93E-33

Supplemental Table 2
Click here to download Supplemental Content (for online-only posting): Brn4 Suppl Table 2.xlsx

Supplementary Table 2: Magenta Module Gene Members

Probe Set*	Gene†	kME	kME p-value
10416588	1300010F03Rik	0.870177415	3.30E-08
10348000	2810459M11Rik	0.913625652	4.59E-10
10542880	4833442J19Rik	0.934764182	2.32E-11
10388042	6330403K07Rik	0.889657498	6.06E-09
10410355	A530054K11Rik	0.853551933	1.14E-07
10457475	Abhd3	0.934680029	2.35E-11
10502951	Acadm	0.872626672	2.71E-08
10347748	Acsl3	0.888262886	6.91E-09
10344725	Adhfe1	0.876708143	1.93E-08
10547386	Adipor2	0.852579396	1.23E-07
10595657	AF529169	0.869093536	3.59E-08
10466925	Ak3	0.908758458	8.20E-10
10401473	Aldh6a1	0.922587141	1.44E-10
10457250	Arhgap12	0.866366325	4.45E-08
10395692	Arhgap5	0.925601469	9.42E-11
10406407	Arrdc3	0.859776553	7.32E-08
10410721	Arsk	0.868552566	3.75E-08
10600755	Arx	0.8696016	3.45E-08
10532538	Asphd2	0.912812072	5.07E-10
10350896	Astn1	0.945841565	3.15E-12
10546977	Atp2b2	0.85217751	1.26E-07
10417124	B930095G15Rik	0.867775501	3.99E-08
10423821	Baalc	0.897952427	2.67E-09
10407286	BC067074	0.880532971	1.39E-08
10379901	Bcas3	0.873821099	2.45E-08
10502451	Bmpr1b	0.866152331	4.52E-08
10553080	Car11	0.883520538	1.07E-08
10442468	Caskin1	0.870167824	3.30E-08
10476355	Chgb	0.880044326	1.45E-08
10417027	Cldn10	0.91597036	3.43E-10
10402473	Clmn	0.952345692	7.95E-13
10578904	Cpe	0.906203955	1.10E-09
10487645	Cpxm1	0.922015714	1.55E-10
10460468	Ctsf	0.876473486	1.97E-08
10514520	Cyp2j9	0.891511091	5.07E-09
10497381	Cyp7b1	0.912038595	5.57E-10
10426921	Dazap2	0.947135795	2.43E-12
10511679	Decr1	0.908907118	8.06E-10
10446596	Dlgap1	0.945363499	3.46E-12
10472809	Dlx1	0.85644367	9.32E-08
10423388	Dnahc5	0.875848496	2.07E-08
10440926	Dnajc28	0.910395331	6.77E-10
10454254	Dtna	0.941753672	6.88E-12
10413932	E130203B14Rik	0.901986687	1.75E-09
10451054	Enpp4	0.933659824	2.77E-11
10445338	Enpp5	0.855273514	1.01E-07

10523845	Ephx4	0.900121937	2.13E-09
10417561	Fam107a	0.952646207	7.43E-13
10369132	Fam184a	0.90817393	8.78E-10
10417620	Fezf2	0.887985106	7.09E-09
10494565	Fmo5	0.871452228	2.98E-08
10563872	Gabra5	0.880581541	1.38E-08
10503334	Gem	0.919271527	2.24E-10
10363173	Gja1	0.937410326	1.49E-11
10346321	Gm10561	0.963384984	4.61E-14
10471945	Gm13476	0.86756889	4.05E-08
10376208	Gm2a	0.904485718	1.33E-09
10390032	Gm5540 /// Acsf2	0.954550694	4.77E-13
10468533	Gpam	0.920599337	1.88E-10
10407803	Gpr137b	0.915787101	3.51E-10
10407792	Gpr137b-ps	0.90954752	7.48E-10
10567355	Gprc5b	0.893594312	4.14E-09
10573626	Gpt2	0.884949184	9.38E-09
10592471	Gramd1b	0.917848427	2.70E-10
10606088	Hdac8	0.928287222	6.36E-11
10512721	Igfbpl1	0.879992237	1.46E-08
10407173	Il6st	0.950228724	1.27E-12
10378681	Inpp5k	0.852302613	1.25E-07
10449266	Itfg3	0.879405697	1.53E-08
10607085	Kcne1l	0.900799576	1.98E-09
10360972	Kcnk2	0.899535511	2.26E-09
10578448	Klkb1 /// Cyp4v3	0.880405074	1.40E-08
10552075	Lgi4	0.892522857	4.60E-09
10564909	Man2a2	0.861111356	6.63E-08
10450025	March2	0.861055276	6.66E-08
10380289	Mmd	0.879505622	1.52E-08
10535938	N4bp2l1	0.951337624	9.96E-13
10456254	Nedd4l	0.902507203	1.65E-09
10407420	Net1	0.882296654	1.19E-08
10429754	Nrbp2	0.868445391	3.78E-08
10408359	Nrsn1	0.885901441	8.60E-09
10591978	Ntm	0.908923663	8.05E-10
10394685	Ntsr2	0.868975578	3.63E-08
10474312	Pax6	0.896490523	3.10E-09
10390103	Pdk2	0.929300129	5.47E-11
10543017	Pdk4	0.891373981	5.14E-09
10404792	Phactr1	0.94385682	4.64E-12
10469867	Pnpla7	0.859028089	7.73E-08
10543004	Pon2	0.85902251	7.73E-08
10601459	Pou3f4	0.857555568	8.60E-08
10361104	Ppp2r5a	0.877798988	1.76E-08
10546421	Prickle2	0.908198503	8.75E-10
10465683	Rab11b-ps2 /// Rab11b	0.855303231	1.01E-07
10354741	Rftn2	0.921163495	1.74E-10
10397030	Rgs6	0.963522778	4.43E-14

10399360	Rhob	0.859070283	7.71E-08
10552156	Rhpn2	0.911943394	5.63E-10
10399696	Rnf144a	0.933268896	2.95E-11
10499854	S100a1	0.85817096	8.23E-08
10367746	Sash1	0.899569885	2.26E-09
10595033	Scg3	0.944133153	4.40E-12
10422598	Sepp1	0.970930968	3.77E-15
10506360	Sgip1	0.871934334	2.86E-08
10476021	Sirpa	0.896910695	2.97E-09
10459866	Slc14a1	0.909075664	7.91E-10
10474141	Slc1a2	0.895087343	3.57E-09
10363563	Slc25a16	0.882184385	1.20E-08
10596718	Slc38a3	0.885237531	9.13E-09
10405605	Smad5	0.910608266	6.61E-10
10399801	Sntg2	0.925633771	9.37E-11
10495285	Sort1	0.91752633	2.81E-10
10382328	Sox9	0.937061343	1.58E-11
10347992	Spata3	0.941951572	6.63E-12
10556509	Spon1	0.888902806	6.51E-09
10546855	Srgap3	0.906807124	1.03E-09
10369615	Srgn	0.899572855	2.26E-09
10592618	Tbcel	0.894352188	3.84E-09
10494007	Them4	0.94322609	5.23E-12
10380285	Tmem100	0.891595641	5.03E-09
10499045	Trim2	0.869683205	3.43E-08
10428536	Trps1	0.909042844	7.94E-10
10419170	Txndc16	0.873239121	2.57E-08
10494428	Txnip	0.922632604	1.43E-10
10399046	Vipr2	0.868320478	3.82E-08
10439542	Zdhhc23	0.908843113	8.12E-10
10482448	Zeb2	0.870323037	3.26E-08
10481401	Zer1	0.906475762	1.06E-09

*Probe set ID for Affymetrix Mouse Gene 1.0 ST microarray.
†For genes with multiple corresponding probes, the probe with the highest kME was included; Probes without a known corresponding gene were not included.

Supplementary Table 2: Black Module Gene Members

Probe Set*	Gene†	kME	kME p-value
10435004	1500031L02Rik	0.853323238	1.16E-07
10582586	1700054N08Rik	0.885632142	8.81E-09
10538408	2410066E13Rik	0.933824439	2.70E-11
10433709	2900011O08Rik	0.857771705	8.47E-08
10483536	4930578N16Rik	0.904981179	1.26E-09
10362363	6330407J23Rik	0.958907908	1.61E-13
10362372	9330159F19Rik	0.928376184	6.28E-11
10377534	A030009H04Rik	0.923487929	1.27E-10
10539669	Add2	0.915416176	3.68E-10
10594631	Aph1b	0.918042334	2.63E-10
10381474	Arl4d	0.946958606	2.52E-12
10368875	Armc2	0.889643276	6.07E-09
10396125	Atl1	0.938154003	1.31E-11
10370651	BC005764	0.93608567	1.86E-11
10576844	BC068157	0.853938524	1.11E-07
10374727	Bcl11a	0.966791555	1.60E-14
10402554	Bcl11b	0.935935009	1.91E-11
10596880	Bsn	0.870823892	3.13E-08
10480492	Cacna1b	0.930021751	4.90E-11
10547322	Cacna1c	0.872418928	2.75E-08
10518812	Camta1	0.959112539	1.52E-13
10430649	Cbx7	0.869270252	3.54E-08
10603362	Ccdc120	0.859132696	7.67E-08
10523297	Ccng2	0.908619167	8.34E-10
10379482	Cdk5r1	0.95504642	4.24E-13
10494069	Celf3	0.977380603	2.46E-16
10457895	Celf4	0.884791849	9.51E-09
10589130	Celsr3	0.91872325	2.41E-10
10395039	Cmpk2	0.874519308	2.32E-08
10521498	Crmp1	0.908876195	8.09E-10
10458046	D0H4S114	0.882795683	1.14E-08
10485550	D430041D05Rik	0.93546736	2.06E-11
10502359	Dapp1	0.853281936	1.17E-07
10582551	Dbndd1	0.882040359	1.22E-08
10404250	Dcdc2a	0.883670123	1.05E-08
10607156	Dcx	0.975597378	5.62E-16
10593384	Dixdc1	0.859387086	7.53E-08
10543058	Dlx5	0.929437305	5.36E-11
10536353	Dlx6	0.899288879	2.32E-09
10403112	Dnahc11	0.858792912	7.86E-08
10532511	E130006D01Rik	0.89013962	5.79E-09
10451786	Efhb	0.864115864	5.29E-08
10514352	Elavl2	0.968615713	8.67E-15
10591706	Elavl3	0.919985995	2.04E-10
10515095	Elavl4	0.926652839	8.09E-11
10416541	Enox1	0.934467342	2.43E-11

10503118	Fam110b	0.858878392	7.81E-08
10401443	Fam161b	0.878806869	1.61E-08
10375167	Fam196b	0.89442895	3.81E-09
10359255	Fam5b	0.930543962	4.52E-11
10351400	Fam78b	0.871742163	2.91E-08
10524941	Fbxo21	0.893032074	4.37E-09
10505030	Fsd1l	0.883861571	1.03E-08
10542200	Gabarapl1	0.877551927	1.80E-08
10472707	Gad1	0.936471324	1.74E-11
10344973	Gdap1	0.950578458	1.18E-12
10438784	Gm606	0.857226058	8.81E-08
10417787	Gng2	0.916838809	3.07E-10
10535021	Gpc2	0.882697457	1.15E-08
10409365	Gprin1	0.865022748	4.93E-08
10508052	Grik3	0.918635641	2.44E-10
10565193	Hdgfrp3	0.891683388	4.99E-09
10512721	Igfbpl1	0.853948626	1.11E-07
10351801	Igsf9	0.881189043	1.31E-08
10588826	Ip6k1	0.865434027	4.78E-08
10469151	Itih5	0.903943073	1.41E-09
10373113	Kif5a	0.943550141	4.92E-12
10372151	Lrriq1	0.904507011	1.33E-09
10424833	Maf1	0.864296564	5.22E-08
10498076	Maml3	0.904815833	1.28E-09
10434629	Map3k13	0.88160615	1.26E-08
10481128	Med22	0.878896564	1.60E-08
10486041	Meis2	0.910535386	6.66E-10
10554655	Mex3b	0.968259234	9.80E-15
10370818	Mex3d	0.884482149	9.78E-09
10382866	Mgat5b	0.895827766	3.31E-09
10350341	Mir181b-1 /// Mir181a-1	0.874277264	2.36E-08
10474361	Mpped2	0.965348457	2.54E-14
10578324	Mtus1	0.881962834	1.23E-08
10368199	Myb	0.860749273	6.81E-08
10479698	Myt1	0.874807338	2.26E-08
10395074	Myt1l	0.860540701	6.92E-08
10372342	Nav3	0.88358881	1.06E-08
10577471	Nek5	0.877360858	1.83E-08
10457820	Nol4	0.98424924	4.74E-18
10397575	Nrxn3	0.992970078	6.91E-22
10375019	Nsg2	0.968144075	1.02E-14
10385203	Odz2	0.879341363	1.54E-08
10585905	Parp6	0.897648635	2.75E-09
10359870	Pbx1	0.935770916	1.96E-11
10500469	Pde4dip	0.954023006	5.40E-13
10498309	Pfn2	0.900204464	2.11E-09
10534085	Phkg1	0.874093033	2.40E-08
10543802	Plxna4	0.943056721	5.40E-12
10357948	Ppp1r12b	0.915153057	3.80E-10

10412066	Rab3c	0.899434393	2.29E-09
10354741	Rftn2	0.854317165	1.08E-07
10448081	Rgmb	0.871263383	3.02E-08
10432362	Rhebl1	0.887816537	7.20E-09
10350742	Rnasel	0.927200855	7.47E-11
10400926	Rtn1	0.925312865	9.81E-11
10522976	Rufy3	0.905179434	1.23E-09
10429944	Scrt1	0.965472496	2.44E-14
10494174	Sema6c	0.975650341	5.49E-16
10557535	Sez6l2	0.916751741	3.11E-10
10416887	Slain1	0.854621552	1.06E-07
10478124	Slc32a1	0.967530621	1.25E-14
10496975	Slc44a5	0.9316207	3.83E-11
10581479	Smpd3	0.884372482	9.88E-09
10476512	Snap25	0.947406635	2.30E-12
10463875	Sorcs3	0.894935337	3.62E-09
10399189	Sp8	0.911932706	5.64E-10
10472930	Sp9	0.948937251	1.67E-12
10423745	Spag1	0.883791912	1.04E-08
10533055	Srrm4	0.920117979	2.01E-10
10490665	Stmn3	0.959467892	1.39E-13
10416090	Stmn4	0.875055875	2.22E-08
10430596	Sun2	0.917334898	2.88E-10
10603843	Syn1	0.870306449	3.26E-08
10547140	Tmcc1	0.87596838	2.05E-08
10504891	Tmeff1	0.882198618	1.20E-08
10347226	Tmem169	0.931624871	3.83E-11
10422518	Tmtc4	0.901910415	1.76E-09
10481949	Traf1	0.907602724	9.37E-10
10607259	Tro	0.874701324	2.28E-08
10518989	Trp73	0.863049208	5.73E-08
10428068	Tspyl5	0.860905482	6.73E-08
10454015	Ttc39c	0.898834218	2.44E-09
10576332	Tubb3	0.883922465	1.03E-08
10361834	Txlnb	0.863521657	5.53E-08
10361055	Vash2	0.936731896	1.67E-11
10468783	Vax1	0.87497153	2.23E-08
10495343	Wdr47	0.928113267	6.53E-11
10357381	Ysk4	0.892926419	4.42E-09
10498720	Zbbx	0.861180745	6.59E-08
10593225	Zbtb16	0.872392512	2.76E-08
10605820	Zc4h2	0.860788108	6.79E-08
10445071	Zfp57	0.919850575	2.08E-10
10497222	Zfp704	0.945907991	3.11E-12
10601492	Zfp711	0.866872432	4.28E-08
10559825	Zfp773	0.898379867	2.55E-09
10449920	Zfp811	0.891858771	4.90E-09

*Probe set ID for Affymetrix Mouse Gene 1.0 ST microarray.

†For genes with multiple corresponding probes, the probe with the highest kME was included; Probes without a known corresponding gene were not included.